SEASONS AND CHAOS IN ECOSYSTEMS

Sergio Rinaldi, Simona Muratori, Yuri Kuznetsov,
Marten Scheffer, and Francesco Doveri
International Institute for Applied Systems Analysis
Laxenburg, Austria

Foreword

Since its foundation IIASA has played an important role in proving the power of dynamical system theory for understanding the behavior of natural and exploited resources.

Insect pest outbreaks in forest ecosystems, selfpurification in rivers, lake management and exploitation of fish stocks, are examples of the research carried out at IIASA in this field. During the development of these studies, a great deal of attention has been paid to the problems of randomness and discontinuity of ecological systems which, indeed, are very often unpredictable and undergo catastrophic transitions. These very complex issues can be nowadays highlighted by suitably combining basic results of bifurcation theory of nonlinear systems and powerful numerical techniques. This is exactly what has been done in Summer 1991 by some scientists who have investigated, within the Dynamic Systems Project, the relationships between seasons and chaos in ecosystems. The present research report combines two journal articles which were published concerning this theme. They show that the strength of the seasons (i.e., the latitude) is a key factor for understanding the strange behavior of the ecosystem and that chaos can be present in an assembly of different communities provided that the rhythm of the seasons suitably interferes with the endogenous rhythms of the biological processes. The first paper by Rinaldi *et al.* studies a general predator–prey model describing the behavior of two interacting populations in a periodic environment. Multiple attractors and catastrophic transitions are proved to exist and the two classical routes to chaos (torns destruction and cascade of period doublings) are numerically detected. The second paper by Doveri *et al.* presents a seasonally perturbed plankton–fish model composed by five compartments: nutrient, algae, zooplankton, young fish, and adult fish. The bifurcation analysis of the model supports the conclusion that the dynamics of plankton communities can easily be chaotic provided that the strength of the season is sufficiently strong. In particular, the paper shows why large

iv

year to year differences in young fish survival need not always be attributable
to external factors like interannual weather variability.

Peter de Jánosi
Director

Seasonality and Chaos in a Plankton–Fish Model

FRANCESCO DOVERI

*Laboratorio di Informatica Territoriale e Ambientale,
Politecnico di Milano, Milan, Italy*

MARTEN SCHEFFER

*Institute of Inland Water Management and Waste Water Treatment,
Lelystad, The Netherlands*

SERGIO RINALDI

CIRITA, Politecnico di Milano, Milan, Italy

SIMONA MURATORI

Politecnico di Torino, Torino, Italy

AND

YURI KUZNETSOV

*Research Computing Centre, Russian Academy of Sciences,
Pushchino, Moscow Region, Russia*

The dynamics of a plankton–fish model comprising phosphorus, algae, zooplankton and young fish are analyzed for different values of average light intensity, phosphorus concentration in the inflow, and adult fish biomass. Light intensity and water temperature are periodically varied during the year, while the other parameters are fixed at realistic values. The analysis is carried out with a continuation method for the study of the bifurcations of periodically forced continuous-time nonlinear systems. The large number of bifurcations of different types indicates that the dynamics of the model can be very complex. In fact, multiplicity of attractors, catastrophic transitions, subharmonics of various periods, cascades of period doublings, and strange attractors arise for suitable values of the parameters. The results are in agreement with the most recent theories on food chain systems and periodically forced predator–prey systems. They also suggest that large year-to-year differences in food chain dynamics need not always be attributable to external factors like interannual weather variability.   © 1993 Academic Press, Inc.

159

1. INTRODUCTION

Historical time series of plant, animal, and human populations are often so irregular that it is hard to imagine that these populations are near an equilibrium. Nevertheless, some sort of periodicity is sometimes detectable in these time series. Examples of this kind are insect–pest outbreaks in forests (Royama, 1984), algae blooms in artificial reservoirs and lakes (Harris, 1986), fluctuations of some animal populations (Schaffer, 1984), dynamics of childhood diseases (Schaffer and Kot, 1985), and many others. Nevertheless, also in these cases, the deviations from a periodic pattern are conspicuous. Such deviations were attributed to various difficulties that arise when collecting data (measurement noise), or to fluctuations of environmental factors influencing the populations (process noise). In other words, scientists believed that, if the absence of measurement and process noise, populations would be constant or periodic and that all deviations from these modes of behavior would be due to random accidents.

The discovery that nonlinear dynamical systems can behave in a purely chaotic way in the absence of exogenous noise sources has radically modified this belief. In other words, it could be that many of the deviations of a population from an equilibrium or a cycle are due to the internal mechanisms of reproduction and growth of the population and not to the influence of external forces. May (1974) was the first to point out this possibility in a study on insect populations with nonoverlapping generations. Since then, the problem of deterministic chaos in population dynamics has been intensely investigated. The analysis of many classical models has proved that chaos may arise for suitable values of the parameters characterizing the population. Among these studies we can recall those on parasitism (May, 1985; Lauwerier and Metz, 1986), competition (Gilpin, 1979), sex (Caswell and Weeks, 1986), and predation (Inoue and Kamifukumoto, 1984; Schaffer, 1988; Rinaldi et al., 1993) and the recent investigations on food chains (Scheffer, 1991; Hastings and Powell, 1991) and on a chemostat with a predator, a prey, and a periodically forced inflowing substrate (Kot et al., 1992). However, detecting chaos from real population data, which are, in any case, affected by some kinds of noise, is, at least, equivocal. Identifying the presence of deterministic chaos in such time series requires the capability of distinguishing between nonchaotic time series affected by noise and chaotic time series affected by noise. Nevertheless, the use of numerical techniques has allowed different authors to conjecture the presence of chaos, for example, in the dynamics of the Canadian Lynx population (Schaffer, 1984), in the growth of some species of trees (Gutierrez and Almiral, 1989), and in certain childhood disease epidemics (Schaffer and Kot, 1985; Olsen, 1987; Kot et al., 1988; Sugihara and May, 1990). As a result population

communities have all the ingredients of strongly nonlinear dynamics (for a debate on the importance of chaos in biology see Schaffer and Kot, 1986; Berryman and Millstein, 1989; Pool, 1989a, b).

This paper is devoted to the study of a model of plankton dynamics in a seasonal environment. In addition to the effects of light, temperature, and nutrients on the planktonic system, we take the impact of planktivorous fish into account. Traditionally, this aspect is rarely considered in plankton models (see, e.g., Jorgensen (1983) for a review), although the dominant influence of fish on plankton in many aquatic systems is now documented by a large number of studies (e.g., Lamarra, 1975; Leah *et al.*, 1980; Cronberg, 1982; Shapiro and Wright, 1984; Reinertsen and Olsen, 1984; Levitan *et al.*, 1985). Field data and laboratory experiments show that the dynamics of the populations coexisting in a water body are rather complex, although some general patterns are mostly identifiable. A well known scenario is the occurrence of a spring bloom of algae follwed by a zooplankton peak inducing a clear water phase, which, subsequently, changes to a more turbid situation with low zooplankton densities (Sommer *et al.*, 1986). In other cases continuing regular density oscillations are found, especially of large Cladocerans (McCauley and Murdoch, 1987). Often, however, field data on plankton show considerable irregularity. Algae do peak in early Summer (blooms), but the amplitude and the time of occurrence of these blooms and subsequent zooplankton peaks are often quite different from one year to the next. The concentration of the limiting nutrient (in general phosphorus), as well as the biomass of young fish feeding on zooplankton, follows a simpler pattern during the year, but these patterns often vary conspicuously and aperiodically through years. In short, recorded time series of phosphorus, algae, zooplankton, and fish clearly point out two characteristic frequencies. A low frequency (1-year period) obviously due to the 1-year periodicity of the environmental factors (light intensity, water temperature, etc.) regulating the growth of all species involved in the process, and a high frequency (1- to 2-month period). Nevertheless, random deviations from the average periodic pattern are not negligible. These deviations have been, until now, explicitly attributed to the unpredictable fluctuations of environmental factors. In other words, algae, zooplankton, and fish populations would have exactly the same pattern repeating each year (periodic solution of "period one") if the environment were perfectly periodic.

With no intention of underestimating the role of the environmental randomness, we present in this paper the results of a study which shows that plankton dynamics can be intrinsically chaotic. This fact could have been somehow conjectured by a naive analogy with the most recent results on periodically forced predator–prey systems (Rinaldi *et al.*, 1993; Kot *et al.*, 1992). But the models discussed in these contributions are not suited for

describing the planktonic system. For this reason we have performed a systematic and detailed analysis of all possible modes of behavior of a more complex model. Our model is composed by five compartments, namely, phosphorus, algae, zooplankton, young fish, and adult fish (the last considered as a parameter) and encapsulates the most important processes (influence of light intensity and nutrient concentration on algal growth, functional response of zooplankton and fish, recycling of phosphorus through excretion, decomposition, and mineralization, temperature dependence of growth, mortality rates, and so forth). The discussion is carried out with respect to three parameters: latitude, phosphorus concentration of the inflow, and fish biomass. Light intensity, water temperature, and recruitment of young fish are taken as periodically varying input functions of the model, while all other parameters are fixed at realistic values. The analysis shows that such a model has very complex dynamics, comprising multiple attractors, catastrophes, subharmonics, and chaos. Multiplicity of attractors can lead to high sensitivity to noise; catastrophes imply conspicuous variations of the populations for small variations of strategic parameters; subharmonics correspond to periodic behavior with long periods (3, 4, ... years); chaos implies no periodicity whatsoever although patterns may look periodic at first sight.

The paper is organized in sections. In the next section we present our model and outline its limitations. In Section 3 the continuation method used to compute the bifurcations of the model is described. In the fourth section we present the results of the analysis in terms of bifurcation curves in two-dimensional parameter spaces. The presence of chaos is detected by means of Poincaré sections which point out the fractal geometry of the attractors. Finaly, in Section 5 we summarize the results and outline the most important directions for further research.

2. Model Description

The model considers the part of the aquatic ecosystem depicted in Fig. 1. Each compartment shown in the figure corresponds to one state variable in the model, except for the biomass of "adult fish," which is kept constant, as is discussed later. Obviously, the variables represent complex groups of species. Assuming that hydrology is constant the formulation of the model is

$$\dot{P} = \delta(P_0 - P) - A\Psi_A + \rho_A m_A^* A + \rho_Z m_Z^* Z + \rho_F m_F^* F \\ + \xi_Z Z\Psi_Z + \xi_F F\Psi_F \tag{1}$$

$$\dot{A} = e_A A\Psi_A - Z\Psi_Z - m_A^* A - \delta A \tag{2}$$

$$\dot{Z} = e_Z Z\Psi_Z - F\Psi_F - V_0\Psi_{V_0} - m_Z^* Z - \delta Z \tag{3}$$

$$\dot{F} = e_F F\Psi_F - m_F^* F + V_0 i(t, L_0) - Fd(t, L_0), \tag{4}$$
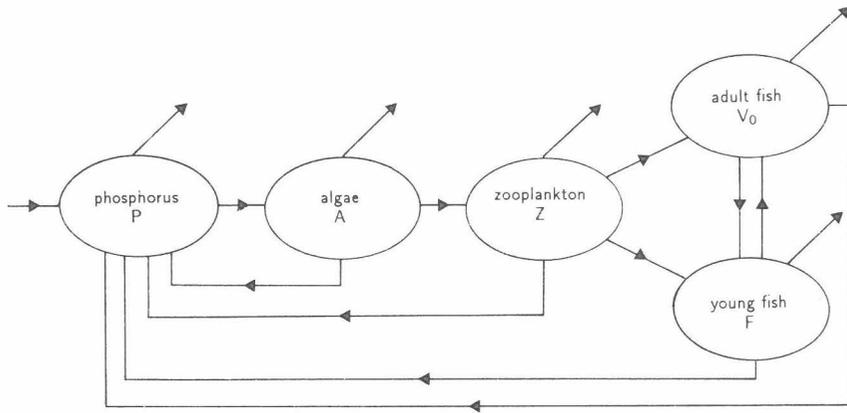
FIG. 1. The flow of material in the phosphorus–plankton–fish model. Connections between the two fish compartments represent recruitment and aging processes. In the model each compartment is described by a single variable and adult fish V_0 is assumed to be constant, while all other variables (P, A, Z, F) are in accordance with a differential equation (mass balance).

where the four functional responses Ψ are given by

$$\Psi_A = \beta_A^* \frac{P}{k_A + P} \cdot \frac{L}{\gamma A + L}$$

$$\Psi_Z = \beta_Z^* \frac{A}{k_Z + A}$$

$$\Psi_F = \beta_F^* \frac{Z}{k_F + Z}$$

$$\Psi_{V_0} = B_{V_0}^* \frac{Z^2}{k_{V_0}^2 + Z^2}$$

and

P = phosphorus concentration

A = algal concentration

Z = zooplankton concentration

F = young fish biomass

V_0 = adult fish biomass

P_0 = phosphorus concentration in the inflow

L_0 = average light intensity

L = light intensity

ρ_A (ρ_Z) (ρ_F) = amount of nutrient released by decomposition of a unit of dead algae (zooplankton) (young fish)

ξ_Z (ξ_F) = amount of phosphorus excreted by zooplankton (fish) per unit of algae (zooplankton) eaten

m_A^* (m_Z^*) (m_F^*) = mortality rate of algae (zooplankton) (young fish)

δ = inverse of retention time

e_A (e_Z) (e_F) = efficiency of algae (zooplankton) (young fish)

$i(t, L_0)$ = recruitment rate of young fish

$d(t, L_0)$ = aging rate of young fish

γ = self-shading capacity of algae

β_A^* = maximum rate of phosphorus uptake

β_Z^* = maximum grazing rate of zooplankton

β_F^* ($\beta_{V_0}^*$) = maximum predation rate of young (adult) fish

k_A, k_Z, k_F, k_{V_0} = half saturation constants (i.e., values of A, Z, F, and V_0 at which the corresponding functional responses are half maximum).

Table I gives the dimensions of parameters, the range of realistic values, and the relevant sources of this information. In all figures which follow phosphorus concentration (P) is in mg P 1^{-1}, while algal (A), zooplankton (Z), and young fish (F) concentrations are in mg dw 1^{-1}. The stars (*) appearing in Eq. (1)–(4) denote a temperature dependence. In accordance with the most commonly used Q_{10} approximation of Arrhenius law, all parameters varying with temperature are assumed to double every 10°. The corresponding values at 20° C are indicated in Table I without *.

Light intensity L and water temperature T are assumed to be sinusoidal functions of t (day),

$$L(t) = L_0 \left(1 + \varepsilon_L \sin \frac{2\pi}{365} t \right)$$

$$T(t) = T_0 \left(1 + \varepsilon_T \sin \frac{2\pi}{365} (t - \tau_T) \right),$$

where $t = 0$ at Spring Equinox. In order to reduce the number of parameters, the average light intensity L_0, inversely related to latitude, has been selected as an independent parameter, while τ_T has been fixed to 80 days and ε_L, T_0, and ε_T have been related through linear regression to L_0 using data of lakes at different latitudes. The result is

$$\varepsilon_L = 2.3027 - 0.0048 L_0$$

$$T_0 = 0.034 L_0$$

$$\varepsilon_T \doteq 0.8 \varepsilon_L = 1.8421 - 0.0038 L_0.$$

TABLE I

The Parameters of the Model, Their Units, Their Minimum and Maximum Values,
and the Sources of Information Supporting These Data

Parameter	Units	Min value	Max value	Source of information
L_0	calc m^{-2} day^{-1}	300	400	Hutchinson, 1957
V_0	mg dw l^{-1}	0.5	3	Scheffer, 1992
P_0	mg P l^{-1}	0	2	Vendegna and Teruggi, 1984
m_A	day^{-1}	0.05	0.4	Scheffer, 1992
m_Z	day^{-1}	0.1	0.25	Scheffer, 1992
m_F	day^{-1}	0.01	0.03	Scheffer, 1992[a]
e_A	mg dw(mg P)$^{-1}$	70	125	Scheffer, 1992[a]
e_Z	—	0.5	0.7	Scheffer, 1992
e_F	—	0.4	0.6	Scheffer, 1992[a]
ρ_A	mg P(mg dw)$^{-1}$	2.85×10^{-3}	4.65×10^{-3}	Scheffer, 1992[a]
ρ_Z	mg P(mg dw)$^{-1}$	2.85×10^{-3}	4.65×10^{-3}	Scheffer, 1992[a]
ρ_F	mg P(mg dw)$^{-1}$	2.85×10^{-3}	4.65×10^{-3}	Scheffer, 1992[a]
ξ_Z	mg P(mg dw)$^{-1}$	4.5×10^{-3}	9.5×10^{-3}	Scheffer, 1992[a]
ξ_F	mag P(mg dw)$^{-1}$	4.5×10^{-3}	7.5×10^{-3}	Scheffer, 1992[a]
γ	calc m^{-2} day^{-1}(mg dw)$^{-1}$ l	120	180	Steemann and Hansen, 1959
δ	day^{-1}	0	0.05	Matsamura and Sakawa, 1980
β_A	mg P day^{-1}(mg dw)$^{-1}$	0.005	0.015	Scheffer, 1992
β_Z	day^{-1}	0.5	0.7	Matsamura and Sakawa, 1980
β_F	day^{-1}	0.10	0.20	Scheffer, 1992[a]
β_{V_0}	day^{-1}	0.4	0.6	Scheffer, 1992
k_A	mg P l^{-1}	0.01	0.03	Matsamura and Sakawa, 1980
k_Z	mg dw l^{-1}	0.05	0.13	Matsamura and Sakawa, 1980
k_F	mg dw l^{-1}	0.25	0.75	Scheffer, 1992[a]
k_{V_0}	mg dw l^{-1}	0.8	1.2	Scheffer, 1992

Note. In all figures of the paper, unless explicitly stated, the parameters are equal to the central value of the range indicated in this table.

[a] and references therein.

In the following we describe briefly the rationale behind the model formulation, concentrating on the less traditional aspects of it.

The phosphorus equation (1) contains the following terms: net input, uptake by algae, release from decomposing algae, zooplankton, and fish and finally excretion by zooplankton and fish. The concentration P_0 is kept constant and is used to set the nutrient level in the system. Seasonal variation in processes like uptake by and release from sediments and aquatic macrophytes are neglected. Nutrient release from decomposing organisms is considered an instantaneous process, and excretion by zooplankton and fish is taken proportional to their consumption rates.

The algal equation (2) consists of a growth term, mortality due to zooplankton grazing, basic mortality, and an outflow from the system. The growth Ψ_A, obviously dependent upon phosphorus concentration, is also

a function of light. The Monod function for light dependence can be easily justified (Cornelli, 1989) and serves to describe the competition effect due to self shading. The grazing Ψ_Z by zooplankton is also written as a Monod formulation (type II functional response).

Zooplankton, in the model, should be thought of as large Cladocerans-like Daphnia species. This group represents the most dominant grazers of algae and is also most vulnerable to fish predation (Scheffer, 1992, and references therein). Concerning the zooplankton equation (3) it should be noted that there are two different predation losses, one for adult fish, and one for "young of the year" fish. Young fish are supposed to have a type II Ψ_F functional response, whereas the adult fish have a type III functional response Ψ_{V_0}, because unlike the young fish, the larger animals are able to switch to alternative prey (Scheffer, 1992).

The equation for fish (4) is probably the least traditional part of the model. Generally, plankton and fish dynamics are not described in the same model. The rationale behind this is that the characteristic time scales of these groups differ quite substantially. This might be true if one focuses on the total biomass of the fish population, but certainly not if the planktivorous capacity is of interest. Young fish of almost all species go through a stage at which they are obligatory planktivores. Therefore, the yearly recruitment, which often gives rise to massive peaks of young fish, causes the predation pressure of the fish community on zooplankton to show a pronounced seasonal peak. Unfortunately, it is not reasonable to put this peak into the model as a forcing function, since it is known that there are large interannual differences in young fish survival, depending on the availability of plankton at the moment that young fish are in their planktivorous stage. Equation (4) shows how this complex interaction with fish is incorporated in the model. The number of adult fish, as mentioned before, is treated as constant with respect to the time scale of interest. Young fish have a consumption dependent biomass growth and a fixed mortality. In addition, there is an input, proportional to the number of adult fish representing recruitment, and an output representing the aging of young fish. Obviously, the latter process would put them in the adult fish class, if this class were modelled dynamically. The input and output of young fish are uniformly spread over some time. The timing of recruitment is especially relevant in this context. It is formulated in such a way that the input process is finished 6 weeks after the temperature reaches $14°$ C, which is the moment that, on average, young fish start to forage heavily on large zooplankters. More precisely, the recruitment function $i(t, L_0)$ is equal to 0.005 for 20 days starting from day $\tau_i = 158 - 0.26L_0$ (typically the beginning of May) and 0 otherwise, while the aging function $d(t, L_0)$ is equal to 0 for 120 days starting from day τ_i, and to 0.05 for the rest of the year.

The model is rather complex compared to traditional models used up to now. Although crude simplifications are made, and many potentially interesting factors are still left out of consideration, the number of parameters is large. This prohibits an extensive analysis over the complete parameter space. After it has been checked that the qualitative behavior of the model is sound for all realistic values of the parameters, the strategy has therefore been to analyze the behavior of the model with respect to just three parameters: the light intensity (L_0), the phosphorus loading (P_0), and the adult fish biomass (V_0). All other parameters are fixed in the middle of the realistic ranges given in Table I.

3. The Method of Investigation

The model, adding the equation $i = 1$ ($t \bmod 1$ year), can be transformed into an autonomous five-dimensional system for which four-dimensional Poincaré section and four-dimensional first return map

$$(P(0), A(0), Z(0), F(0)) \mapsto (P(1), A(1), Z(1), F(1))$$

can be defined (Arnold, 1982; Guckenheimer and Holmes, 1983). This map specifies the values $P(1)$, $A(1)$, $Z(1)$, $F(1)$ that the four state variables have at the end of the year, once the values $P(0)$, $A(0)$, $Z(0)$, $F(0)$ that the same variables have at the beginning of the year are known. Fixed points of the kth iterate of the map correspond to periodic solutions with period k years. We refer to these points as period k fixed points. It should be noted that a periodic solution with period k corresponds to a k-ple of period k fixed points of the Poincaré map. Closed and regular curves (invariant tori) on the Poincaré section correspond to quasi-periodic solutions, while irregular invariant sets (strange attractors) correspond to chaotic solutions. Fixed points of the Poincaré map can bifurcate at some parameter values. In the following we discuss bifurcations in two-dimensional parameter spaces and therefore talk of bifurcation curves. In all our figures we display only bifurcations involving at least one attractor because only these bifurcations are of biological interest.

We use the following notation for fixed point codimension one bifurcations.

$f^{(k)}$—flip (period doubling) bifurcation curve. For parameter values on this curve the map has a period k fixed point with a multiplier $\mu_1^{(k)} = -1$. When this curve is approached, a stable cycle of period k loses stability and smoothly becomes a stable cycle of period $2k$.

$t^{(k)}$—tangent (fold) bifurcation curve. For parameter values on this curve the map has a period k fixed point with a multiplier $\mu_1^{(k)} = 1$. On this curve a stable and an unstable cycle of period k collide and disappear.

The bifurcation curves presented in the following section have been computed by means of a continuation method interactively supported by the program LOCBIF developed by A. Khibnik, Yu. A. Kuznetsov, V. Levitin, and E. Nikolaev at the Research Computing Centre of the USSR Academy of Sciences at Pushchino. The method can be briefly described as follows (Khibnik, 1990a, b). Each bifurcation curve is computed by projecting a one-dimensional manifold located in the six-dimensional space (P, A, Z, F, p_1, p_2) on the (p_1, p_2) plane, where p_1 and p_2 are two parameters (for example, P_0 and L_0). The manifold is determined by the four fixed point equations and by a bifurcation condition imposed on the multipliers of the fixed point. This condition is written using the characteristic polynomial $\det(J - \mu I)$, where J is the Jacobian matrix of the proper iterate of the Poincaré map at point (P, A, Z, F) and I is the 4×4 unit matrix. More precisely, the bifurcation conditions are $\det(J + I) = 0$ for flip bifurcation and $\det(J - I) = 0$ for tangent bifurcation. In the program LOCBIF the bifurcation curves are computed by means of an adaptive prediction–correction continuation procedure with tangent prediction and Newton correction. All relevant derivatives, as well as the Poincaré map, are evaluated numerically.

4. ANALYSIS OF THE RESULTS

In this section we present and interpret bifurcation curves in the parameter spaces (P_0, L_0) and (V_0, L_0). These curves are only some of the bifurcation curves we have obtained. In particular, we do not display bifurcation curves involving only unstable modes of behavior, because they are of no biological interest. (They are needed only if one likes to fully understand the global bifurcation structure of the system from a purely formal point of view (Kuznetsov *et al.*, 1992).) We also do not show bifurcation curves that we have detected only in very small regions of the parameter space because we are not sure whether they correspond to relevant phenomena. For these reasons, the analysis is not complete and the modes of behavior we point out are only samples of the dynamics of our plankton–fish model. Nevertheless, these samples are quite interesting and refer to characteristic phenomena that we have checked to be robust with respect to parameter perturbations.

In order to be as clear as possible, we present the results in three different subsections dedicated, respectively, to multiplicity of attractors, catastrophes, and chaos.

4.1. *Multiplicity of Attractors*

It is already known (Muratori and Rinaldi, 1989; Scheffer, 1992) that even the most rudimentary food chain model composed of a prey, a predator, and a constant superpredator has multiple attractors in the absence of seasonalities. On the other hand, it was pointed our recently (Rinaldi *et al.*, 1993) that periodic variations of environmental factors can easily give rise to multiple attractors even in the simple predator–prey models which have only one attractor in a constant environment. Thus, multiplicity of attractors may also be expected in our plankton–fish model, which is more complex than a simple food chain and has many periodically varying factors.

Figure 2 shows two sets of bifurcation curves in the parameter space (P_0, L_0). In Fig. 2a we have two branches of a tangent bifurcation of period 1. In the shaded region delimited by the two curves, the system has two stable cycles of period 1 and an unstable cycle of period 1. When a bifurcation curve $t^{(1)}$ is crossed coming from inside the shaded region, one of the two stable cycles collides with the unstable one and disappears. Thus, in the shaded region we have coexistence of two distinct stable cycles of period 1, while outside that region we have only one stable mode of behavior. Figure 3 shows the two coexisting attractors for point 1 of Fig 2a. In both cases algae peak three times per year and zooplankton peaks (essentially) two times per year, but the amplitudes of the oscillations are quire different. Of course, each of these attractors has its own basin of attraction, so that, in the presence of heavy intermittent noise, the system will randomly visit the two attractors.
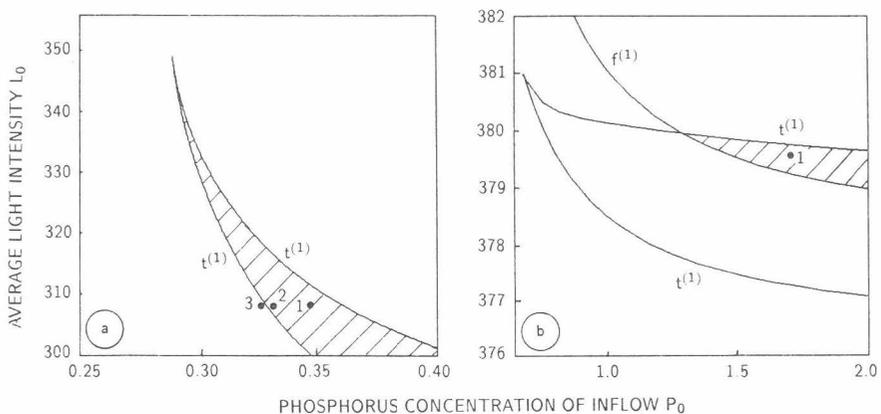
FIG. 2. Bifurcation curves in the two-parameter space (P_o, L_0) with $V_0 = 1.00$. (a) Tangent bifurcations of period 1 (on the two curves $t^{(1)}$, a stable and an unstable periodic solution of period 1 collide and disappear). (b) Tangent and flip bifurcations of period 1 (crossing the flip curve $f^{(1)}$ from the left to the right a stable periodic solution of period 1 loses stability and becomes a stable periodic solution of period 2). Units are as in Table I.

DOVERI ET AL.
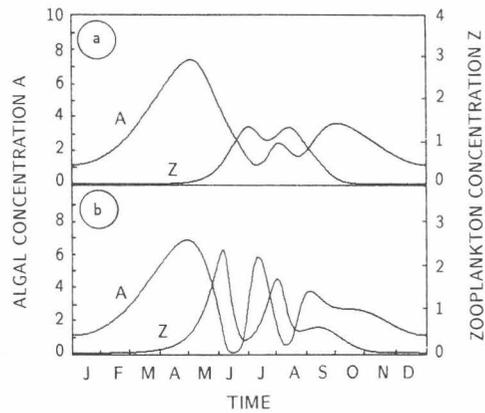
FIG. 3. Coexistence of attractors. Two stable periodic (a) and (b) solutions of period 1 corresponding to the same parameter values, $P_0 = 0.346$. $L_0 = 308$, $V_0 = 1.00$. See point 1 of Fig. 2a. In the second attractor (b) algae and zooplankton blooms are much more marked. Concentrations are in mg dw l^{-1}.

Figure 2b shows another set of bifurcation curves, namely flip of period 1 and tangent of period 1. When the flip bifurcation curve $f^{(1)}$ is crossed from below, a stable cycle of period 1 loses stability and becomes a stable cycle of period 2. In the shaded region of Fig. 2b we have two attractors: a cycle of period 1 and a cycle of period 2. Figure 4 shows these two attractors for point 1 of Fig. 2b. Recognizing that the second attractor is not a cycle of period 1 requires a close look: this is because point 1 in Fig. 2b is situated near the flip bifurcation curve $f^{(1)}$ where cycles of period 2 degenerate into cycles of period 1. The period 2 behavior shown in Fig. 4b is an example of subharmonic behavior. The occurrence of subharmonics in
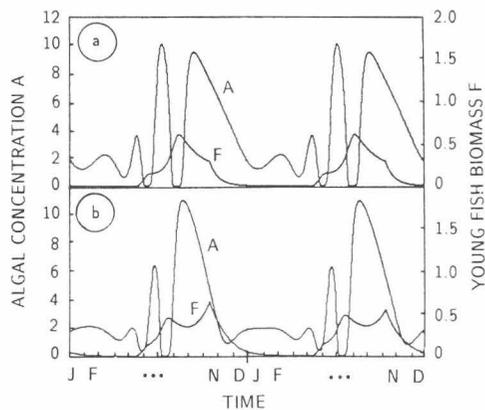
FIG.4. Coexistence of attractors. The attractor (a) is a cycle of period 1, while the attractor (b) is a cycle of period 2. The parameter values are $P_0 = 1.710$, $L_0 = 379.5$, $V_0 = 1.00$. See point 1 of Fig. 2b. Algal concentration and young fish biomass are in mg dw l^{-1}.

the model suggests that plankton communities can vary periodically with period $k = 2, 3, ...$ years even if environmental factors do vary periodically with period 1.

4.2. *Catastrophes*

Macroscopic transitions can easily occur for small variation of a parameter in a nonlinear system with multiple attractors (May, 1977). Perhaps the best known example (Noy-Meir, 1975) in population dynamics is the crash of food chain systems for an increase of the exploitation rate of the top predator (adult fish in our case). On the other hand, it has been recently ascertained (Rinaldi *et al.*, 1993) that seasonalities can favor catastrophic transitions in simple predator–prey models. Thus, it may be expected that our plankton–fish model can also undergo substantial transitions when parameters like phosphorus or adult fish biomass are slightly perturbed. Confirmations of this conjecture can be found in Figs. 5 and 6. In each one of these figures the two stable modes of behavior are shown. In Fig. 5 the transition is obtained by lowering the phosphorus concentration of the inflow (see points 2 and 3 in Fig. 2a). Since the catastrophe is associated with a tangent bifurcation of period 1, the system "jumps" from a cycle of period 1 (Fig. 5a) to another cycle of period 1 (Fig. 5b). Nevertheless, the two cycles are different, the first one having much more pronounced oscillations. In Fig. 6 the catastrophe is obtained by increasing the biomass of adult fish so that a curve of tangent bifurcations of period 3 (see curve $t^{(3)}$ of Fig. 12, below) is crossed. The attractor,
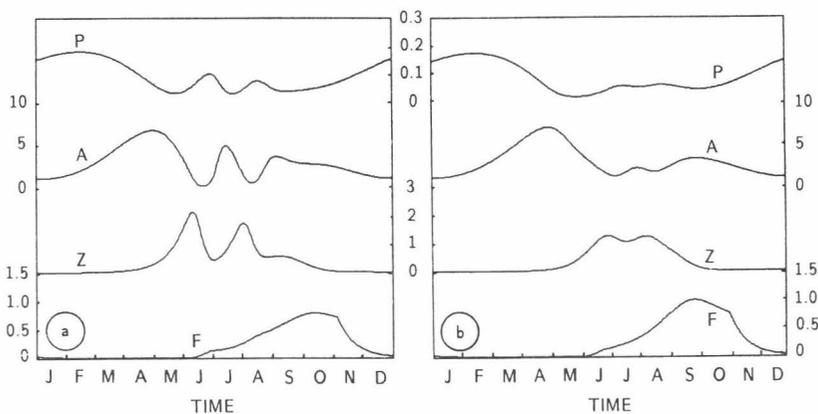
FIG. 5. Catastrophic transitions. Two stable cycles of period 1 for the same average light intensity ($L_0 = 308$) and adult fish biomass ($V_0 = 1.00$), and for slightly different phosphorus concentrations of the inflow ($P_0 = 0.330$ in (a) and $P_0 = 0.325$ in (b)). See points 2 and 3 in Fig. 2a. Lowering the concentration of phosphorus in the inflow generates a catastrophic transition from a cycle with marked algae and zooplankton blooms to a smoother cycle.
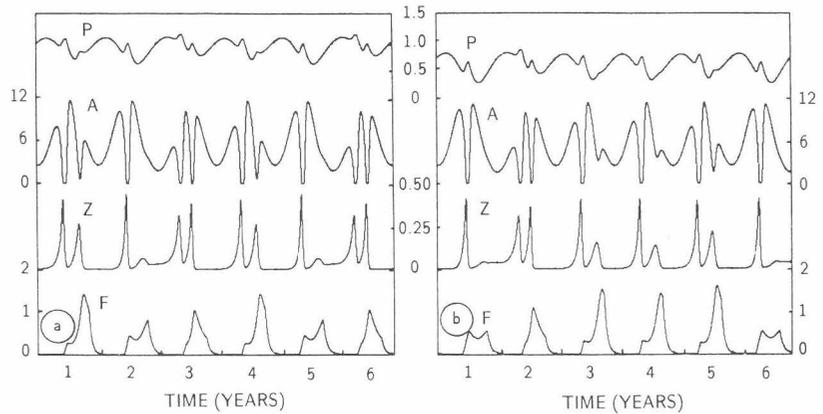
FIG. 6. Catastrophic transitions. A stable cycle of period 3 and a strange attractor for the same average light intensity ($L_0 = 340.7$) and phosphorus concentration of inflow ($P_0 = 1.00$) and for slightly different values of adult fish biomass ($V_0 = 2.115$ in (a) and $V_0 = 2.150$ in (b)). Increasing the adult fish biomass gives rise to a catastrophic transition from a cycle to a strange attractor.

just before the bifurcation, is therefore a cycle of period 3 (Fig. 6a), while, just after the bifurcation, the system behaves aperiodically on a strange attractor (Fig. 6b). Note that the aperiodicity of the strange attractor is more easily seen in the dynamics of the higher trophic levels (fish) than, for instance, in phosphorus and algae.

4.3. Deterministic Chaos

Deterministic chaos has been shown to be possible in many simple continuous-time population models. Food chain systems have been proved
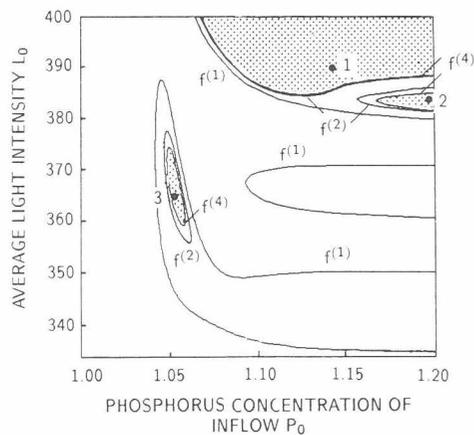
FIG. 7. Flip bifurcations curves $f^{(1)}$, $f^{(2)}$, $f^{(4)}$ in the two-parameter space (P_0, L_0), with $V_0 = 1.00$. In the three dotted regions chaotic behavior is possible (see also the next three figures showing the strange attractors of points 1, 2, and 3).

to be chaotic even in the constant parameter case (Hogeweg and Hesper, 1978; Scheffer, 1991; Hastings and Powell, 1991). The classical predator–prey model can become chaotic when one of its parameters is varied periodically (Inoue and Kamifukumoto, 1984; Schaffer, 1988; Toro and Aracil, 1988; Allen, 1989; Kuznetsov *et al.*, 1992; Rinaldi *et al.*, 1993) and the lowest amplitude of the seasonal variation needed to generate chaos can become quite small if there are many periodic factors acting on the system (Rinaldi and Muratori, 1993). Finally, a chemostat model composed by nutrient, prey, and predator has also been shown to be chaotic for suitable amplitudes of the periodically varying inflow concentration of the
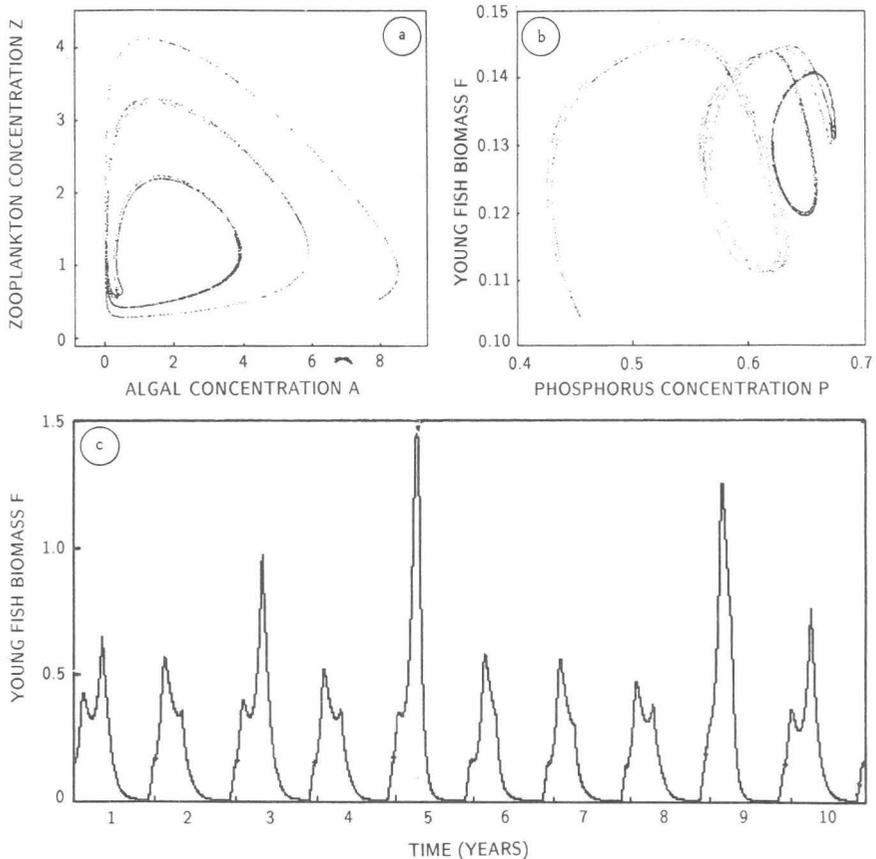
FIG. 8. Chaotic behavior of the model. Parts (a) and (b) show two projections of the strange attractor on the Poincaré section. The fractal structure of the attractor is clearly displayed. Part (c) shows the irregular fluctuations of the biomass of young fish during a period of 10 years (the year starts the first day on which all the young fish forage on zooplankton). The parameter values identifying the attractor are $P_0 = 0.887$, $L_0 = 390$, and $V_0 = 1.00$. See point 1 of Fig. 7.

nutrient (Kot *et al.*, 1992). It would, therefore, be at least surprising if our plankton–fish model were not chaotic in some subregions of the parameter space.

Figure 7 shows a complete set of flip bifurcation curves in the parameter space (P_0, L_0) and three distinct regions in which chaos may arise. If the phosphorus concentration of the inflow P_0 is slowly increased over time and the average light intensity L_0 is fixed at a high value (*e.g.*, $L_0 = 390$), the model predict that the standard period 1 periodic solution wil first bifurcate into a period 2 periodic solution (on curve $f^{(1)}$) and then, for a slightly larger value of P_0, again double its period (on curve $f^{(2)}$) and
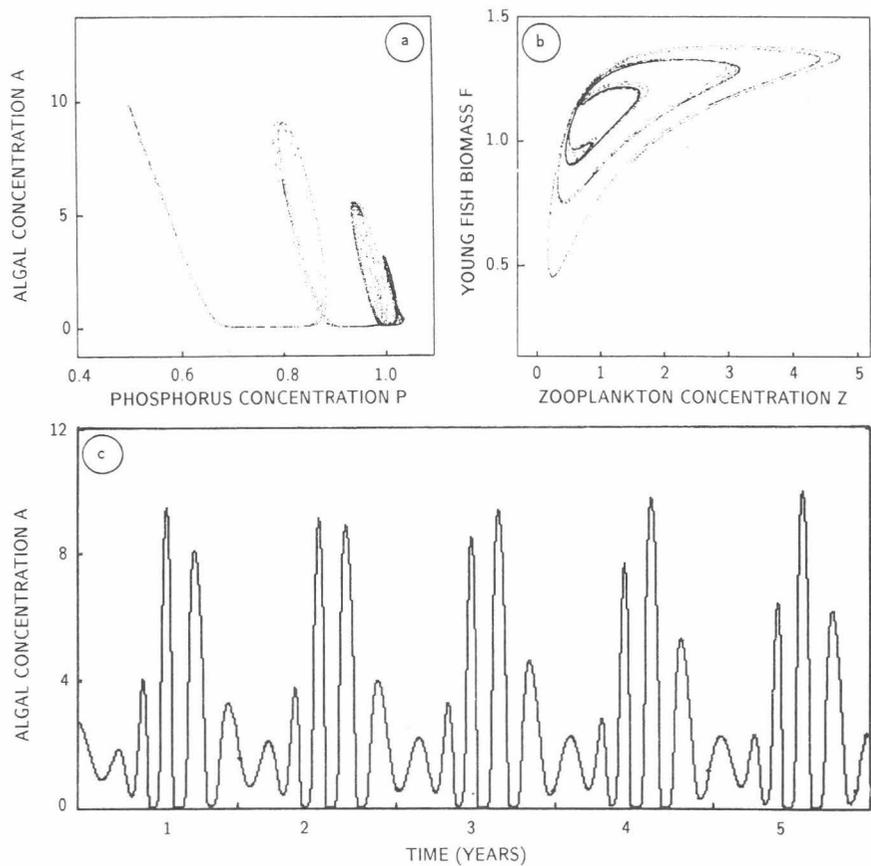
FIG. 9. Chaotic behavior of the model. Parts (a) and (b) show two different projections of the strange attractor. Part (c) shows the irregular fluctuations of the algal concentration during a period of 5 years (the year starts the first day on which all the young fish forage on zooplankton). Chaos can be detected by comparing the minor blooms of each year. The parameter values identifying the attractor are $P_0 = 1.192$, $L_0 = 384$, and $V_0 = 1.00$. See point 2 of Fig. 7.

continue in this manner until the periodicity is lost. At that point the attractor becomes a genuine chaotic attractor. This region of chaos is characterized by high concentrations of phosphorus (eutrophic lakes) so that algae are not nutrient limited. This is equivalent to saying that plankton and fish are independent of phosphorus concentration and that the model, in fact, reduces to a three stage food chain. The amplitudes of the light and temperature seasonal variations in this food chain are rather small because L_0 is high. Nonetheless, the existence of chaos in this region of the parameter space is not a surprise, since food chain systems can be chaotic in a constant environment especially if growth rates are high. The closed region of chaos at lower values of P_0 and L_0 is also interesting
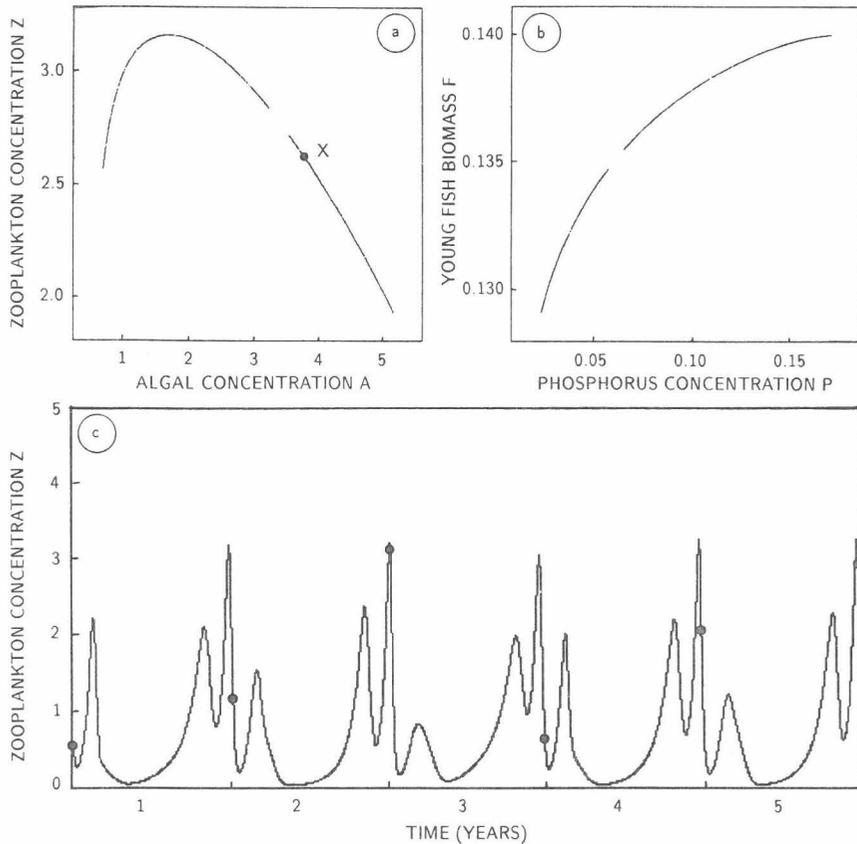
FIG. 10. Chaotic behavior of the model. Parts (a) and (b) show two different projections of the strange attractor. The fractal structure of the attractor cannot be perceived at this scale (see the next figure for two successive zoomings). Part (c) shows the irregular fluctuations of the zooplankton concentration during 5 successive years starting the day on which all the youhg fish forage on zooplankton. The parameter values identifying the attractor are $P_0 = 0.390$, $L_0 = 364.8$, and $V_0 = 1.00$. See point 3 of Fig. 7.
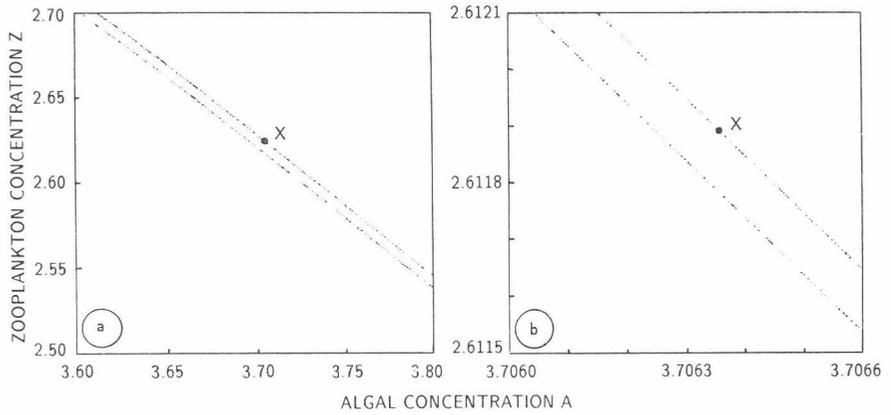
FIG. 11. The selfsimilarity property of a strange attractor. When zooming into a small square around point X of Fig. 10a, the "line" representing the attractor appears as the double line of (a). Zooming more deeply on point X the upper "line" of (a) becomes the double line of (b).

because it shows that chaos can be obtained either by increasing or by decreasing the concentration of nutrient, a result similar to that found by Kot *et al.* (1992) for a much simpler model. Finally, Fig. 7 shows that there are very large regions, in particular in eutrophic lakes, where the system behaves periodically with period 2.

The strange attractors corresponding to points 1, 2, and 3 in Fig. 7 are shown in Figs. 8, 9, and 10. The upper part ((a) and (b)) of these figures shows two different projections of the Poincaré sections. Each dot in these figures is a sample of the variables indicated on the axis, taken the same
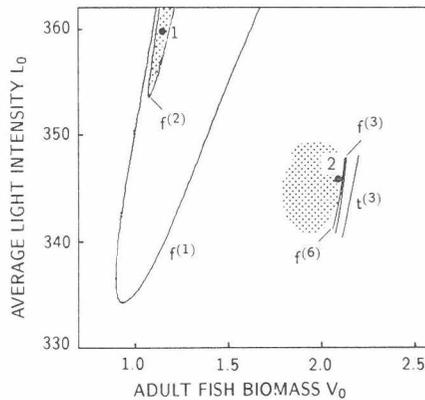
FIG. 12. Flip and tangent bifurcation in the two-dimensional parameter space (V_0, L_0) with $P_0 = 1.00$. The strange attractors present in the shaded regions are obtained through cascade of period doublings $f^{(1)}, f^{(2)}, \dots$ and $f^{(3)}, f^{(6)}, \dots$ (see also the next two figures, showing the strange attractors of points 1 and 2).

day once a year 500 times. The lower part (c) of each figure shows the corresponding time series of one of the populations: as already remarked for Fig. 6b, the irregularity of the attractor is at first sight more evident for fish than for algae. An explanation for the large interannual differences in fish becomes apparent if one samples the zooplankton population on the first day on which the young fish cohort is fully foraging on large zooplankton (see dots in Fig. 10c). The density of zooplankton, which is of critical importance to fish at this life stage, is highly variable. The match or mismatch of the appearance of young fish and the peak in their food availability has been suggested as the main cause of the huge year-to-year differences in young fish survival of natural fish populations (Cushing and Dickson, 1976; Cushing, 1982). Our analysis suggests that in addition to
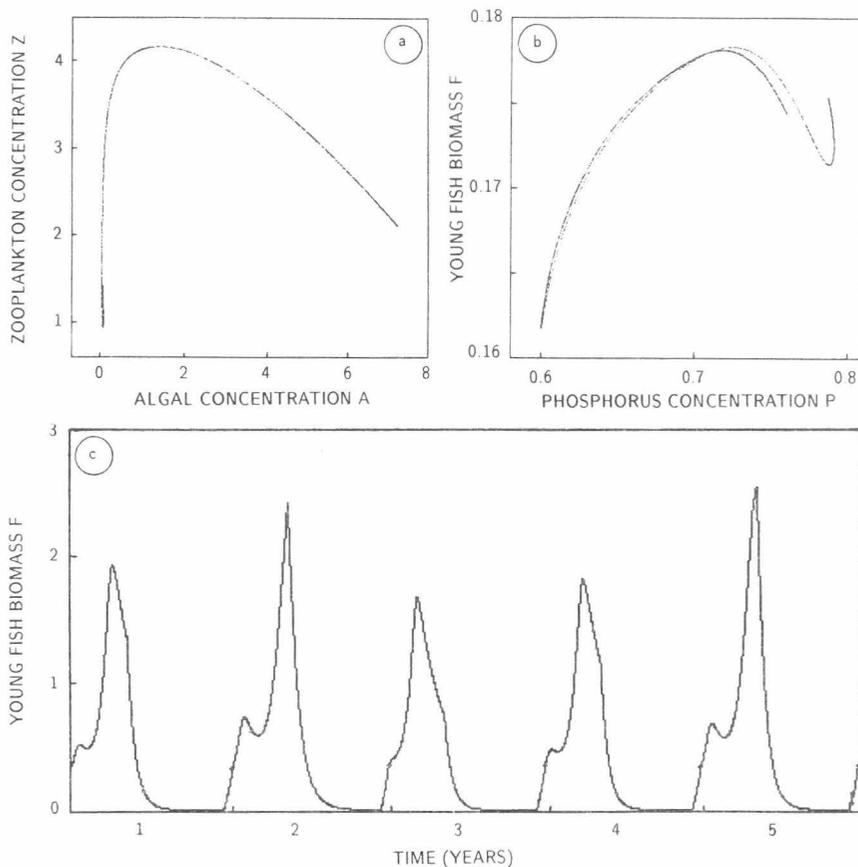
FIG. 13. Chaotic behavior of the model. Parts (a) and (b) show two different projections of the strange attractor of point 1 of Fig. 12 ($V_0 = 1.15$, $L_0 = 360$, $P_0 = 1.00$). Part (c) shows the irregular fluctuations of young fish biomass during 5 successive years.

DOVERI ET AL.

meteorological variability the intrinsic chaos in the aquatic ecosystem is a likely cause of this mechanism.

The fractal geometry of the attractors is very clear in Fig.s 8 and 9, while Fig. 10 displays an attractor which, at first glance, seems to represent some kind of quasi-periodicity (behavior on torus). Nevertheless, the fractal nature of this attractor can be revealed by changing the scale of observation.

Figure 11 illustrates the results of two successive zoomings into the attractor and points out the classical selfsimilarity property of fractal sets.

To conclude our analysis of chaos, we show in Fig. 12 two other period doubling routes to chaos in the parameter space (V_0, L_0). The figure indicates that adult fish biomass might be a critical control variable, because an increase of this variable can cause either the appearance or the
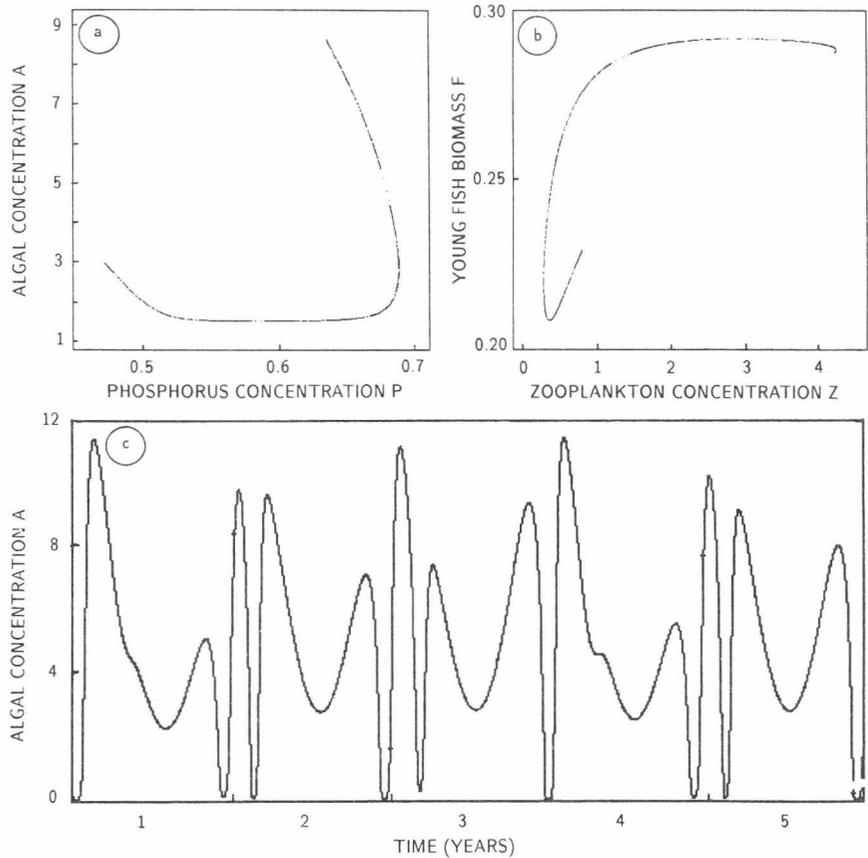
FIG. 14. Chaotic behavior of the model. Parts (a) and (b) show two different projections of the strange attractor of point 2 of Fig. 14 ($V_0 = 2.11$, $L_0 = 345.9$, $P_0 = 1.00$). In (c) the randomness of the algae blooms is particularly evident on the secondary peaks.

disappearance of chaos. The strange attractors corresponding to points 1 and 2 of Fig. 12 are shown in Figs. 13 and 14. Also in these cases, the variability of the young fish peaks is greater than that of the algal blooms.

5. CONCLUDING REMARKS

We have shown in this paper that the variability of the yearly patterns of plankton and fish populations (usually attributed to some environmental randomness) can be a direct consequence of the biological and physical processes characterizing the model. This conclusion is based upon the results obtained by analyzing the stable modes of behavior of a model with periodically varying light intensity, water temperature, and fish recruitment and aging. From a technical point of view, the analysis has required the study of the bifurcations of a periodically forced four-dimensional dynamical system: a quite difficult problem that could not have been solved by standard simulation techniques. We have used, instead, a package implementing a powerful continuation method producing flip and tangent bifurcation curves of periodic solutions of any period. The package also detects "codimension two" bifurcation points, a fact that has not been emphasized in the paper but which is of strategic importance for successfully organizing the analysis (Kuznetsov *et al.*, 1992).

Some of the results we have obtained confirm many of the conclusions recently obtained by different authors who have analyzed the dynamics of simple ecological models. The chaos predicted by our model in eutrophic lakes at low latitudes seems to be originated by the possibility that three stage food chains behave aperiodically even in a constant environment (Scheffer, 1991; Hastings and Powell, 1991). The existence of subharmonics and of strange attractors obtained through cascade of period doublings is in line with the analysis carried out in Rinaldi *et al.* (1993), while the rarity of quasi-periodic behavior is perhaps due to the high ratio between the period (1 year) of the forcing functions and the period (1–2 months) of the autonomous oscillations of phytoplankton–zooplankton communities.

There are many caveats when interpreting the results of rather abstract models like the one discussed in this paper in terms of real world biology. Nonetheless, a number of significant inferences can be made. First, the analysis shows that the normal seasonal cycle of light and temperature can easily lock the relatively fast cycling plankton system into yearly repeated pattern. This result will probably be in accordance with general biological intuition. More remarkable is the observation that the interplay of the season with the intrinsic rhythms caused by food chain interactions can give rise to more irregular patterns. Sometimes the same seasonal pattern may repeat every 2 or 3 years, but more often no repetition whatsoever is found. The pattern is chaotic, although, at first glance, the time series often

look more or less like yearly repeated patterns. This mix of regularity and randomness is, of course, in perfect accordance with observations on seasonal dynamics in nature. However, the real world randomness will, no doubt, also be caused by external perturbations like yearly differences in weather. Nevertheless, it can be stated that observed interannual differences in the ecosystem dynamics need not always be attributable to weather or other external forces. The detected kind of deterministic irregularity offers a good explanation of a phenomenon that has bothered aquatic ecologists for many years: the extremely large year-to-year variation in young fish survival. Although the generated zooplankton patterns often look rather similar in different years, the timing of their peaks appears to vary. Since the timing of fish spawning is triggered by temperature, and not by food availability, this can cause the young fish to be born in a period of either very high or extremely low food abundance, resulting in large differences in survival. The fact that "time shift irregularities" causing this match–mismatch process typically arise from the model suggests that it might be impossible to properly relate the natural variation in recruitment success to weather conditions.

The relationship between the investigated control parameters and the occurrence of phenomena like chaos, catastrophes, and subharmonics in the model is rather complex, but some broad patterns can be detected. The results suggest, for instance, that oligotrophic systems tend to show regular, yearly repeating, seasonal patterns. Chaos arises only in more eutrophic situations. The temperature–light regime of northern countries seems also to be in favor of yearly repeating patterns. The model generates chaos more easily in conditions associated with warm climates. Of course, these conclusions are only based on observations of the behavior in a limited part of the parameter space and should therefore be interpreted with care.

Obviously, the work presented in this paper is merely a starting point for further research. The bewildering range of behavior suggests that a detailed analysis of simplified submodels might be informative. On the other hand, many sources of seasonal variation are still left out of consideration, and the effects of including these extra perturbations would be worth studying. The search for patterns predicted by the model in real world data sets (Sugihara and May, 1990) seems especially challenging. However, in view of the noisy character of most ecological data this is an ambitious target.

References

ALLEN, J. C. 1989. Are natural enemy populations chaotic? *in* "Estimation and Analysis of Insect Populations" (L. McDonald, B. Manly, J. Lockwood, and J. Logan, Eds.), pp. 190–205, Lectures Notes in Statistics, Vol. 55, Springer–Verlag, Berlin.

ARNOLD, V. I. 1982. "Geometrical Methods in the Theory of Ordinary Differential Equations," Springer-Verlag, New York.

BERRYMAN, A. A., AND MILLSTEIN, J. A. 1989. Are ecological systems chaotic—and if not, why not? *Trends Ecol. Evol.* **4**, 26–28.

CASWELL, H., AND WEEKS, D. E. 1986. Two-sex models: Chaos, extinction, and other dynamic consequences of sex, *Am. Nat.* **128**, 707–735.

CORNELLI, E. 1989. "Modelli dinamici non lineari di crescita di popolazioni algali," Master's thesis, Politecnico di Milano, Milan, Italy. [in Italian]

CRONBERG, G. 1982. Changes in the phytoplankton of lake Trummen included by restoration, *Hydrobiologia* **86**, 185–193.

CUSHING, D. H. 1982. "Climate and Fisheries," Academic Press, London.

CUSHING, D. H., AND DICKSON, R. R. 1976. The biological response in the sea to climate changes, *Adv. Mar. Biol.* **14**, 1–22.

GILPIN, M. E. 1979. Spiral chaos in a predator-prey model, *Am. Nat.* **113**, 306–308.

GUCKENHEIMER, J., AND HOLMES, P. 1983. "Nonlinear Oscillations, Dynamical Systems and Bifurcations of Vector Fields," Springer-Verlag, New York.

GUTIERREZ, E., AND ALMIRAL, H. 1989. Tempral properties of some biological systems and their fractal attractors, *Bull. Math. Biol.* **51**, 785–800.

HARRIS, G. P. 1986. "Phytoplankton Ecology, Structure, Function and Fluctuation," Chapman & Hall, London.

HASTINGS, A., AND POWELL, T. 1991. Chaos in a three species food chain, *Ecology* **72**, 869–903.

HOGEWEG, P., AND HESPER, B. 1978. Interactive instruction on population interactions, *Comput. Biol. Med.* **8**, 319–327.

HUTCHINSON, G. E. 1957. "A Treatise on Limnology," Vol. I, "Geography, Physics and Chemistry," Wiley, New York.

INOUE, M., AND KAMIFUKUMOTO, H. 1984. Scenarios leading to chaos in a forced Lotka–Volterra model, *Prog. Theor. Phys.* **71**, 930–937.

JORGENSEN, S. E. 1983. Modeling the ecological processes, *in* "Mathematical Modeling of Water Quality: Streams, Lakes and Reservoirs" (G. T. Orlob, Ed.), pp. 116–149, Wiley, Chichester/New York/Brisbane/Toronto/Singapore.

KHIBNIK, A. I. 1990a. LINLBF: A program for continuation and bifurcation analysis of equilibria up to codimension three, *in* "Continuation and Bifurcations: Numerical Techniques and Applications" (D. Roose, B. de Dier, and A. Spence, Eds.), pp. 283–296, Kluwer, Netherlands.

KHIBNIK, A. I. 1990b. Numerical methods in bifurcation analysis: Parameter continuation approach, *in* "Mathematics and Modelling" (Y. G. Zarhin and A. D. Bazykin, Eds.), pp. 162–197, Center of Biological Research of the USSR Academy of Sciences, Puschino. [in Russian]

KOT, M., SCHAFFER, W. M., TRUTY G. L., GRASER, D. J., AND OLSEN, F. L. 1988. Changing criteria for imposing order, *Ecol. Model.* **43**, 75–110.

KOT, M., SAYLER, G. S., AND SHULTZ, T. W. 1992. Complex dynamics in a model microbial system, *Bull. Math. Biol.* **54**, 619–648.

KUTZNETSOV, YU. A., MURATORI, S., AND RINALDI, S. 1992. Bifurcations and chaos in a periodic predator–prey model, *Int. J. Bifurcations and Chaos* **2**, 117–128.

LAMARRA, V. A., JR. 1975. Digestive activities of carp as major contributor to the nutrient loading of lakes, *Verh. Int. Verein. Limnol.* **19**, 2461–2468.

LAUWERIER, H. A., AND METZ, J. A. J. 1986. Hopf bifurcation in host–parasitoid models, *IMA J. Math. Appl. Med. Biol.* **3**, 191–210.

LEAH, R. T., MOSS, B., AND FORREST, D. E. 1980. The role of predation in causing major changes in the limnology, *Int. Rev. Ges. Hydrobiol.* **65**, 223–247.

LEVITAN, C., KERFOOT, C., AND DE MOTT, W. R. 1985. Ability of Daphnia to buffer trout lakes agains periodic nutrient input, *Verh. Int. Verein. Limnol.* **22**, 3076–3082.

MATSAMURA, T., AND SAKAWA, Y. 1980. Non-linear analysis of nitrogen cycle in aquatic ecosystems, *Int. J. Systems Sci.* **7**, 803–816.

MAY, R. M. 1974. Biological populations with nonoverlapping generations: Stable points, stable cycles and chaos, *Science* **186**, 645–647.

MAY, R. M. 1977. Thresholds and breakpoints in ecosystems with a multiplicity of stable states, *Nature (London)* **269**, 471–477 .

MAY, R. M. 1985. Regulation of population with non-overlapping generations by microparasites: A purely chaotic system, *Am. Nat.* **125**, 573–584.

MCCAULEY, E., AND MURDOCH, W. W. 1987. Cyclic and stable populations: Plankton as a paradigm, *Am. Nat.* **129**(1), 97–121.

MURATORI, S., AND RINALDI, S. 1989. A dynamical system with Hopf bifurcation and catastrophes, *Appl. Math. Comp.* **29**, 1–15.

NOY-MEIR, I. 1975. Stability of grazing systems: An application of predator–prey graphs, *J. Ecol.* **63**, 459–483.

OLSEN, L. F. 1987. Low dimensional strange attractors in epidemics of childhood diseases in Copenhagen, Denmark, *in* "Chaos in Biological Systems" (H. Degn, A. V. Holden, and L. F. Olsen, Eds), NATO ASI Series, Ser. A. Vol. 138, Plenum, New York.

POOL, R. 1989a. Is it chaos, or is it just noise? *Science* **243**, 25–28.

POOL, R. 1989b. Ecologists flirt with chaos, *Science* **243**, 310–313.

REINERTSEN, H., AND OLSEN, Y. 1984. Effects of fish elimination on the phytoplankton community of a eutrophic lake, *Verh. Int. Verein. Limnol.* **22**, 649–657.

RINALDI, S., AND MURATORI, S. 1993. Conditioned chaos in predator–prey models, *Ecol. Model.*, to appear.

RINALDI, S., MURATORI, S., AND KUZNETSOV, YU. A. 1993. Multiple attractors, catastrophes and chaos in seasonally perturbed predator–prey communities, *Bull. Math. Biol.* **55**, 15–35.

ROYAMA, T. 1984. Population dynamics of the spruce budworm *Choristoneura fumiferana*, *Ecol. Monogr.* **54**, 429–462.

SCHAFFER, W. M. 1984. Stretching and folding in Lynx fur returns: Evidence for a strange attractor in nature? *Am. Nat.* **124**, 798–820.

SCHAFFER, W. M. 1988. Perceiving order in the chaos of nature, *in* "Evolution of Life Histories of Mammals" (M. S. Boyce, Ed.), pp. 313–350, Yale Univ. Press, New Haven, CT.

SCHAFFER, W. M., AND KOT, M. 1985. Nearly one dimensional dynamics in a simple epidemic, *J. Theor. Biol.* **112**, 403–427.

SCHAFFER, W. M., AND KOT, M. 1986. Chaos in ecological systems: The goals that Newcastle forgot, *Trends Ecol. Evol.* **1**, 58–63.

SCHAFFER, W. M., OLSEN, L. F., TRUTY, G. L., FULMER, S. L., AND GRASER, D. J. 1988. Periodic and chaotic dynamics in childhood infections, *in* "From Chemical to Biological Organization" (M. Markus, S. Muller, and G. Nicolis, Eds.), pp. 331–347, Springer-Verlag, Berlin.

SCHEFFER, M. 1991. Should we expect strange attractors behind plankton dynamics and if so, should we bother? *J. Plankton Res.* **13**, 1291–1305.

SCHEFFER, M. 1992. Fish and nutrients interplay determines algal biomass, *Oikos* **62**, 271–282.

SHAPIRO, J., AND WRIGHT, D. I. 1984. Lake restoration by biomanipulation—Round Lake, Minnesota, *Freshwater Biol.* **14**, 371–383.

SOMMER, U., GLIWICZ, Z. M., LAMPERT, W., AND DUNCAN, A. 1986. The PEG-model of seasonal succession of planktonic events in fresh waters, *Arch. Hydrobiol.* **106**, 433–471.

STEEMAN, E., AND HANSEN, V. K. 1959. Light adaption in marine phytoplankton populations and its interrelations with temperature, *Physiol. Plant.* **12**, 353–370.

SUGIHARA, G., AND MAY, R. M. 1990. Nonlinear forecasting as a way of distinguishing chaos from measurement error in time series, *Nature (London)* **344**, 734–741.

TORO, M., AND ARACIL, J. 1988. Qualitative analysis of system dynamics ecological models, *Syst. Dyn. Rev.* **4**, 56–80.

VENDEGNA, V., AND TERUGGI, S. 1984. Modello dei rapporti tra zooplankton e alghe, *Acqua e Aria* **1**, 13–28. [in Italian]

MULTIPLE ATTRACTORS, CATASTROPHES AND CHAOS IN SEASONALLY PERTURBED PREDATOR–PREY COMMUNITIES

■ SERGIO RINALDI
CIRITA,
Politecnico di Milano,
20133 Milano, Italy

■ SIMONA MURATORI
Centro Teoria dei Sistemi,
CNR, Politecnico di Milano,
20133 Milano, Italy

■ YURI KUZNETSOV
Research Computing Centre,
Russian Academy of Sciences,
Pushchino, Moscow Region,
142292, Russia

A classical predator–prey model is considered in this paper with reference to the case of periodically varying parameters. Six elementary seasonality mechanisms are identified and analysed in detail by means of a continuation technique producing complete bifurcation diagrams. The results show that each elementary mechanism can give rise to multiple attractors and that catastrophic transitions can occur when suitable parameters are slightly changed. Moreover, the two classical routes to chaos, namely, torus destruction and cascade of period doublings, are numerically detected. Since in the case of constant parameters the model cannot have multiple attractors, catastrophes and chaos, the results support the conjecture that seasons can very easily give rise to complex population dynamics.

1. Introduction.   The study of ecological systems driven by periodic external forces is of great importance since, with almost no exception, population communities are imbedded in periodically varying environments. Temperature variations strongly influence the reproduction rate of bacteria during the day, moon and tide cycles regulate migration rates of numerous species in aquatic and terrestrial ecosystems, light intensity controls photosynthesis during the seasons, hunting perturbs game stocks once a year. It is therefore quite natural to try to identify the functional role that seasons play in the behaviour of population communities. In particular, a basic problem is to understand if the magnitude of the seasonal variations is related to the complexity of the system. Indeed, it has been known since long ago that the nonlinear mechanical and electronic systems described by Duffing and Van der Pol equations have a very simple dynamic behaviour in the constant

parameter case, but become very complex (multiplicity of attractors, catastrophes and chaos) when they are periodically perturbed (Gucken-heimer and Holmes, 1986). Another important example in a different field is the classical SEIR epidemic model which has a globally stable equilibrium in the constant parameter case and a great number of modes of behaviour in the periodically varying case (Schwartz and Smith, 1983; Aron and Schwartz, 1984; Kot *et al.*, 1988; Olsen *et al.*, 1988).

In this paper we prove that the Rosenzweig–MacArthur predator–prey model, composed of a logistic prey and a Holling's type predator, is also very sensitive to seasonality. In the constant parameter case the model has a supercritical Hopf bifurcation and therefore has only one mode of behaviour for each combination of the parameters: a globally stable equilibrum or a globally stable limit cycle. For small magnitudes of the seasonal variations of the parameters the equilibrium is replaced by a periodic solution with the same period of the perturbation (say, period 1), while the limit cycle is, in general, replaced by a quasi-periodic solution (torus). Nevertheless, if the parameter values are such that the period of the limit cycle of the unperturbed system is approximately k times bigger than the period of the forcing function ($k =$ integer), then even a small periodic perturbation of a parameter can give rise to "phase-locking", i.e. to stable period k periodic solutions (called subharmonics). This well-known phenomenon (Guckenheimer and Holmes, 1986) is particularly relevant (and therefore easy to detect numerically) for $k = 2$ and $k = 3$. Period 2 and 3 subharmonics can coexist with the basic period 1 solution as well as with quasi-periodic solutions or with strange attractors obtained through torus destruction. Obviously, the presence of two (or more) attractors, each one having its own basin of attraction, makes the system particularly sensitive to random disturbances. Moreover, some of the bifurcations characterizing the system (for example, tangent and flip bifurca-tions) are such that small variations of a parameter can entail "catastrophic transitions" between different attractors. Finally, for high magnitudes of the seasonal variations the period 2 and 3 subharmonics can very easily undergo a cascade of period doublings ending in a strange attractor. Some of these attractors are quite similar to those discovered by Ueda for the periodically perturbed Duffing equation (Guckenheimer and Holmes, 1986).

This is not the first contribution on periodically forced ecosystems. Discrete-time models (maps), in which the unit time step coincides with the period of the forcing function, have been used to show that quasi-periodic and chaotic solutions are possible in population dynamics (see, for example, May, 1974; Kot and Schaffer, 1984; Lauwerier and Metz, 1986). Models of this kind are very easy to handle and can give rise to spectacular dynamics, in particular when the map is non-invertible as in the famous case of seasonally breeding organisms with nonoverlapping generations (May, 1974). More

interesting continuous time models with periodically varying parameters have been used to show that seasonality can support coexistence of competing species (Cushing, 1980; De Mottoni and Schiaffino, 1981; Smith, 1981; Butler *et al.*, 1985; Namba, 1986), and that periodic Lotka–Volterra predator–prey systems can have a great variety of periodic solutions (Cushing, 1977; Bardi, 1981; Cushing, 1982). Nevertheless, these studies are somehow incomplete, because they do not touch the problem of deterministic chaos. On the contrary, more recent contributions on second order periodically varying predator–prey systems (Inoue and Kamifukumoto, 1984; Schaffer, 1988; Toro and Aracil, 1988; Allen, 1989; Kuznetsov *et al.*, 1992) deal with such a problem and are much closer, at least in spirit, to the present analysis. Specific comments on these contributions can be found in the following sections. Here it suffices to say that the analysis presented in this paper is much more accurate and complete and allows one to synthetically interpret the results. Some interesting analogies can also be found in a very recent work (Kot *et al.*, 1992) on a third order chemostat model with periodically varying concentration of the inflowing substrate.

Finally, we would like to mention that the analysis of a number of recorded time series of seasonally perturbed plant, animal and human populations seems to confirm the existence of the above nonlinear phenomena (Sugihara and May, 1990). Subharmonics of period 2, 3 and 8 days, as well as phase-locking with the moon cycle, have been found by analysing the abundance of reef fishes influenced by tides (Robertson *et al.*, 1990). A low dimensional strange attractor has been ascertained in the Canadian Lynx population by applying Taken's method to the 200 year long time series of number of skins shipped by the Hudson's Bay Company (Schaffer, 1984), while higher dimensional strange attractors have been detected in plant populations through the analysis of tree-rings (Gutierrez and Almiral, 1989). But the most convincing and detailed analysis showing evidence of chaos in a periodically perturbed population is, without doubt, the study of childhood diseases which are strongly influenced by the seasonality of the contact rates induced by the Summer and Christmas vacations in schools (Kot *et al.*, 1988; Olsen *et al.*, 1988). Other examples can be found in the broad area of food chain and food web systems which comprises forest ecosystems with recursive insect pest outbreaks, and aquatic ecosystems with chaotic algae blooms seasonally triggered by light intensity. Nevertheless, we would like to stress that the ultimate goal of this paper is only to show that the analysis of a classical predator–prey model supports the conjecture that seasons can generate very complex ecosystems dynamics, comprising catastrophes and chaos. The reinforcement of this conjecture through the analysis of field data and laboratory experiments is certainly a much more ambitious and difficult task.

2. The Model and the Six Seasonality Mechanisms.   The model we discuss in this paper is the classical Rosenzweig–MacArthur predator–prey model used in the last 20 years to interpret the behaviour of many predator–prey communities, namely:

$$\dot{x} = x\left[r\left(1 - \frac{x}{K} \right) - \frac{ay}{b+x} \right] \tag{1}$$

$$\dot{y} = y\left[e\,\frac{ax}{b+x} - d \right] \tag{2}$$

where the six parameters r, K, a, b, d, e are positive and x and y are the numbers of individuals of prey and predator populations or suitable (but equivalent) measures of their density or biomass. In the absence of predators ($y=0$) the rate of growth of prey per unit of biomass, namely $r(1 - x/K)$, decreases with x. This is the standard assumption of *logistic growth* of populations (Verhulst, 1845) which accounts for competition for food and space among individuals of the same species and for increased mortality at high density due, for example, to higher chances of epidemics at higher frequency of encounters among individuals. The *intrinsic growth rate r* describes the exponential growth of the prey population at low densities, while the *carrying capacity K* is the prey biomass at equilibrium in the absence of predators. The intrinsic growth rate and the carrying capacity increase with the quality and amount of food available to the prey population and can therefore undergo synchronous periodic variations during the year.

The function:

$$q(x) = \frac{ax}{b+x} \tag{3}$$

appearing in equations (1) and (2) is the type 2 *functional response* proposed by Holling (Holling, 1965), which is, by far, the most commonly used in these kind of studies. It represents the prey biomass destroyed by each predator in one unit and can be justified as follows (for a more detailed interpretation see Metz and van Batenburg, 1985). Let us assume that the *searching time*, namely the time the predator spends to find a unit of prey is inversely proportional to prey density, i.e. s/x, where s is a suitable parameter. If the time needed by each predator to handle one unit of prey is h and all other activities (resting time) of the predator occupy a fraction u of its time, we can write:

$$\frac{s}{x}\,q(x) + hq(x) + u = 1$$

from which equation (3) follows with:

$$a = \frac{1-u}{h} \quad b = \frac{s}{h}. \tag{4}$$

Thus, $q(x)$ is a concave saturating function and a is the *maximum harvest rate* of each predator, while b is the *half saturation constant*, namely the density of prey at which the predation rate is half maximum. Finally, the parameter e in equation (2) is a simple conversion factor, called *efficiency*, that specifies the number of newly born predators for each captured prey, while d is the predator *death rate* per capita.

Of course, the parameters must be time-varying if relevant environmental factors periodically fluctuate in time. For simplicity we consider only sinusoidal perturbations so that for any periodic parameter p in equations (1) and (2) we write:

$$p = p_0(1 + \varepsilon \sin 2\pi t)$$

where p_0 is the average value of p and ε is the "degree" of seasonality (notice that εp_0 is the magnitude of the perturbation). Obviously, $0 \leqslant \varepsilon \leqslant 1$ because p cannot be negative: $\varepsilon = 0$ corresponds to absence of seasonality, while $\varepsilon = 1$ means that the maximum value of the parameter is twice its average value.

Real predator–prey communities are characterized by many seasonality mechanisms so that many, if not all, parameters of model (1), (2) vary periodically. Moreover, these periodic variations are often not in phase, because, even when the different seasonality mechanisms have a common physical origin, their influence reaches its maximum at different times. For example, light intensity and water temperature influencing in different ways phytoplankton–zooplankton communities are out of phase of 1 or 2 months in relatively large lakes, although they both depend upon the sun cycle. In order to avoid too heavy an analysis, we only deal with "elementary" seasonality mechanisms, namely with phenomena that entail periodic variations of a single parameter in model (1), (2) or periodic but synchronous variations of two parameters. For this aim, we identify six elementary mechanisms denoted by (i), (ii), . . . , (vi) in the following. The first one entails the synchronous variation of the intrinsic growth rate r and of the carrying capacity K, while all others imply the periodic variation of one parameter.

(i) *Amount of food available to prey* (r, K).   The intrinsic growth rate r in (1) is the difference between basic birth and death rates of the prey. Hence r increases with the amount of food available to the prey community, so that $r = r_0(1 + \varepsilon \sin 2\pi t)$. Since, on the contrary, the prey intraspecific competition (r/K) is not influenced by the amount of food available to the prey it follows that $K = K_0(1 + \varepsilon \sin 2\pi t)$.

(ii) *Prey intraspecific competition* (K).   Surplus of prey mortality at high densities due to competition for special niches or to epidemics can be enhanced in some seasons. If this is the case, the carrying capacity varies periodically, i.e. $K = K_0(1 + \varepsilon \sin 2\pi t)$.

(iii) *Caloric content of the prey* (e).   If the caloric content of the prey varies during the year, like in some plant–herbivore communities, the energy available to the predator for reproduction varies consistently. Hence the efficiency varies periodically, i.e. $e = e_0(1 + \varepsilon \sin 2\pi t)$.

(iv) *Predator exploitation* (d).   The periodic presence of a superpredator exploiting the predator community gives rise to periodic variations of the predator death rate, i.e. $d = d_0(1 + \varepsilon \sin 2\pi t)$. Phytoplankton–zooplankton communities with first year class fish feeding on zooplankton during the Summer and tree–insect pest systems controlled by migratory insectivores are examples of this class.

(v) *Predator and prey mimicry* (b).   When the degree of mimicry of the prey (predator) is not constant during the year or when variations of the habitat facilitate the escape or the capture of the prey in some specific season, the parameter identifying the searching time in equation (4) varies periodically. This implies [see equation (4)] that the half saturation constant varies in the same way, i.e. $b = b_0(1 + \varepsilon \sin 2\pi t)$.

(vi) *Predator resting time* (a).   If the resting time of the predator fluctuates during the year, as in populations characterized by some degree of diapause, the parameter u in (4) varies periodically. Thus the maximum harvest rate of the predator varies in the same manner, i.e. $a = a_0(1 + \varepsilon \sin 2\pi t)$.

The only "single parameter" perturbation we have excluded in our analysis is that of the intrinsic growth rate r, because we have not found an interesting biological interpretation for it. In this respect we must point out that the analysis carried out in Inoue and Kamifukumoto (1984), Toro and Aracil (1988) and Allen (1989) refers exactly to this case. Moreover, the discussion in Inoue and Kamifukumoto (1984) is mainly focused on the influence of the frequency of the forcing function, which is classical in mechanics and electronics but has very little meaning in ecology, while in Toro and Aracil (1988) and Allen (1989) only the results of a few simulations are shown. On the contrary, the discussion in Schaffer (1988) (corresponding to our third elementary mechanism) is more systematic and points out that chaos can be obtained through torus destruction. This is confirmed by our analysis which, nevertheless, shows that the period doubling route to chaos is also present, as was already proved for the fifth elementary mechanism in Kuznetsov *et al.*

(1992) and for a third order chemostat model composed by limiting substrate, heterotrophic prey and holozoic predator in Kot *et al.* (1992).

3. The Constant Parameter Case.   In the absence of seasonality ($\varepsilon = 0$), system (1), (2) is an autonomous second order system where all parameters and state variables are nonnegative. The analysis of the local stability of its equilibria (May, 1972) shows that there is a *Hopf* bifurcation at:

$$K = b\,\frac{ea - d}{ea - d} \tag{5}$$

and a *transcritical* bifurcation at:

$$K = b\,\frac{d}{ea - d}. \tag{6}$$

The Hopf bifurcation is always supercritical [the computation of its Liapunov number is relatively easy if one considers the orbitally equivalent system obtained by multiplying equations (1), (2) by $(b + x)$] and the asymptotic period of the appearing limit cycle is:

$$T_H = 2\pi \left(\frac{K}{rbd}\right)^{1/2}. \tag{7}$$

Moreover, the limit cycle does not bifurcate since it is unique (Cheng, 1981; Wrzosek, 1990). Thus the parameter space is partitioned into three regions separated by the manifolds (5) and (6). For all combinations of the parameters there is a single attractor which is globally stable in the first quadrant as indicated in Fig. 1. More precisely, for sufficiently high values of the carrying capacity K, the attractor is a stale limit cycle. For decreasing values of K this cycle shrinks and disappears through a Hopf bifurcation. Then the attractor is a stable equilibrium which is positive for intermediate values of K and trivial (absence of predator population) for low values of K.

4. Method of Investigation.   For $\varepsilon > 0$ system (1), (2) adding the equation $\dot{t} = 1$ (t mod 1), can be transformed into an autonomous three-dimensional system for which a Poincaré section and first return map $(x(0), y(0)) \rightarrow (x(1), y(1))$ can be defined (Arnold, 1982; Guckenheimer and Holmes, 1986). Fixed points of the kth iterate of the map correspond to periodic solutions (cycles) of equations (1) and (2) with period k (we will refer to these points as *period k fixed points*). Closed and regular invariant curves of the Poincaré map correspond to quasi-periodic solutions (*invariant tori*), while irregular invariant sets correspond to chaotic solutions (*strange attractors*).
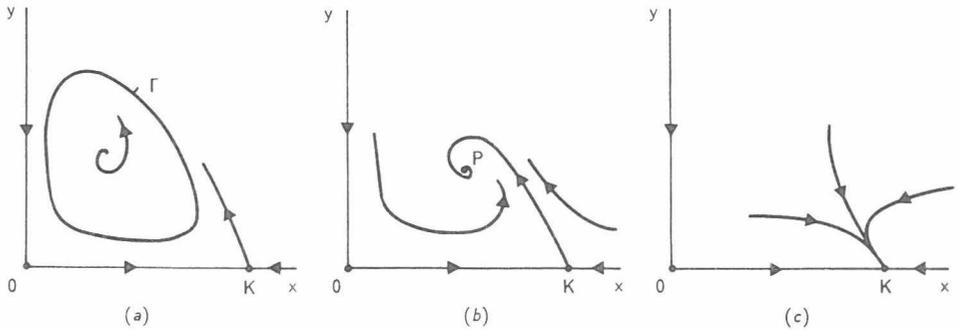
Figure 1. Phase portraits of system (1), (2) in the case of constant parameters: (a) $K > b(ea+d)/(ea-d)$: the attractor is the cycle Γ; (b) $bd/(ea-d) < K < b(ea+d)/(ea-d)$: the attractor is the equilibrium P; (c) $K < bd/(ea-d)$: the attractor is the trivial equilibrium $(K, 0)$.

Non-saddle (i.e. attracting or repelling) and saddle cycles of period k of system (1), (2) can bifurcate at some parameter values. We use the following notation for the corresponding fixed point codimension one bifurcation curves.

$h^{(k)}$—Hopf (Neimark–Sacker) bifurcation curve. For parameter values on this curve the map has a period k fixed point with a pair of multipliers on the unit circle: $\mu_{1,2}^{(k)} = e^{\pm i\omega}$, $\omega > 0$. When curve $h^{(k)}$ is crossed, an attracting (repelling) cycle of period k bifurcates into an attracting (repelling) quasi-periodic solution and a repelling (attracting) cycle of period k.

$t^{(k)}$—tangent (fold) bifurcation curve. For parameter values on this curve the map has a period k fixed point with a multiplier $\mu_1^{(k)} = 1$. When this curve is crossed, a saddle and a non-saddle cycle of period k collide and disappear.

$f^{(k)}$—flip (period doubling) bifurcation curve. For parameter values on this curve the map has a period k fixed point with a multiplier $\mu_1^{(k)} = -1$. When this curve is crossed a saddle (non-saddle) cycle of period k bifurcates into a non-saddle (saddle) cycle of period k and a saddle (non-saddle) cycle of period $2k$.

The behaviour of the system for parameter values close to these curves is described in Arnold (1982) and Guckenheimer and Holmes (1986). It is worthwhile noticing that tangent and flip bifurcations always involve saddle cycles, while Hopf bifurcations are only concerned with attractors and repellors. Moreover, Hopf bifurcations always involve an attractor, while tangent and flip bifurcations sometimes do not. Although all curves $h^{(k)}, t^{(k)}, f^{(k)}$ are needed if one likes to fully understand the structure of the bifurcations of a dynamical system, only those concerning attractors are useful to classify the asymptotic modes of behaviour of the system. In the following, in order to

facilitate the biological interpretation of the results, we will not display bifurcation curves which do not refer to attractors. Readers interested in the bifurcation structure of the model can refer to Kuznetsov *et al.* (1992), where the bifurcation curves corresponding to our fifth elementary mechanism are fully displayed.

The bifurcation curves presented in the next section have been computed by means of a continuation method interactively supported by the program LOCBIF developed by the third author and by A. Khibnik, V. Levitin and E. Nikolaev at the Research Computing Centre of the U.S.S.R. Academy of Sciences at Pushchino.

The method can be briefly described as follows (see Khibnik, 1990a,b). Each bifurcation curve is computed by projecting a one-dimensional manifold located in the four-dimensional space (x, y, p_1, p_2) on the (p_1, p_2)-plane, where p_1 and p_2 are two parameters of (1), (2). The manifold is determined by the two fixed point equations and by a bifurcation condition imposed on the multipliers of the fixed point. This condition is written using the characteristic polynomial $\det(A - \mu I)$, where A is the Jacobian matrix of the Poincaré map at point (x, y) and I is the unit matrix. More precisely, the bifurcation conditions are the following:

$$
\begin{aligned}
R[\det(A - \mu I), \det(\mu A - I)] &= 0 \quad \text{(for \textit{Hopf} bifurcation),} \\
\det(A - I) &= 0 \quad \text{(for \textit{tangent} bifurcation),} \\
\det(A + I) &= 0 \quad \text{(for \textit{flip} bifurcation),}
\end{aligned}
$$

where $R[\cdot,\cdot]$ stands for the *resultant* of two polynomials (Lancaster and Tismenetsky, 1985). In the program LOCBIF the bifurcation curves are computed by means of an adaptive prediction–correction continuation procedure with tangent prediction and Newton correction. All relevant derivatives, as well as the Poincaré map, are evaluated numerically. The program LOCBIF also produces phase portraits of the Poincaré map, continues fixed points in any (x, y, p_1)-space and detects codimension one bifurcations.

5. Bifurcation Curves.   In this section we present and discuss the bifurcation curves of system (1), (2) for the six elementary seasonality mechanisms identified in Section 2. The reference values of the parameters are the following:

$$
e = K = 1 \quad r = d = 2\pi \quad a = 2.2\pi \quad b = 0.3. \tag{8}
$$

For these values, the system oscillates on a limit cycle [K is slightly bigger than $b(ea + d)/(ea - d)$, see equation (5)], and the period of the cycle (evaluated numerically) is $T = 1.85$. Thus, in the parameter space we are not too far from Hopf bifurcations (5) and from $k = 2$ resonances, i.e. values of parameters

giving rise to a cycle of period two times bigger than the period of the forcing function. Actually, the reference values of the parameters have been tuned intentionally in this way, because these are the most favourable conditions to point out periodic and quasi-periodic behaviour, as well as phase-locking of a periodically forced dynamical system. The reader interested in the analysis of the bifurcations of system (1), (2) in other regions of the parameter space can refer to Kuznetsov *et al.* (1992), where the fifth seasonality mechanism is discussed in some more detail.

For each seasonality mechanism the discussion is carried out with respect to two parameters. The first is the degree of seasonality ε, which varies from 0 to 1, and the second is the average value of the periodically varying parameter, i.e. K_0 (with $r_0 = 2\pi \cdot K_0$) in case (i), K_0 in case (ii), e_0 in case (iii), and so on. All other parameters are kept constant at their reference value (8). The second parameter varies in a range that contains the value for which the unperturbed system has a Hopf bifurcation [easily computable from (5)] and the resonant value for which the period of the limit cycle for $\varepsilon = 0$ is equal to 2.

The six diagrams (i), (ii), . . . , (vi) of Fig. 2 display the bifurcation curves of system (1), (2) for the corresponding six seasonality mechanisms. Five bifurcation curves are drawn on these diagrams, namely, $h^{(1)}, h^{(2)}, f^{(1)}, f^{(2)}$ and $t^{(2)}$, the last one composed by two branches ($t_1^{(2)}$ and $t_2^{(2)}$). These bifurcation curves are present in all cases, but curve $h^{(2)}$ cannot be seen in cases (i), (ii), (iii) and (vi) because of the particular range of the parameter. The curves $f^{(1)}, f^{(2)}$ and $t^{(2)}$ are not complete, because the branches not involving attractors have been disregarded. The bifurcation curves $f^{(4)}$ and $f^{(8)}$ have also been obtained but they are not shown in Fig. 2 because they almost coincide with $f^{(2)}$. Nevertheless, they must be kept in mind because they clearly indicate one of the two routes to chaos (i.e. cascade of period doublings).

If we compare the six diagrams 2(i), . . . , 2(vi) we immediately recognize that turning the fourth and fifth upside down we obtain six topologically equivalent diagrams. This fact is very important and clearly indicates that the six seasonality mechanisms give rise to the same phenomena. Let us therefore consider and interpret in detail the qualitative bifurcation diagram of Fig. 3 which is equivalent to those of Fig. 2, but contains, for the sake of clarity, the bifurcation curves $f^{(4)}$ and $h^{(4)}$. The parameter p_0 of this diagram is directly [in cases (i), (ii), (iii) and (vi)] or inversely [in cases (iv) and (v)] related to the average value of the periodically varying parameter. On the p_0-axis there is point H [computable from (5)] corresponding to the Hopf bifurcation of the unperturbed system. Below that point, the attractor of the unperturbed system is an equilibrium, while above it the attractor is a limit cycle. Thus, for small values of ε and below point H we have period 1 periodic solutions, while for small values of ε and above point H we have quasi-periodic solutions. Consistently, a bifurcation curve $h^{(1)}$ rooted at point H separates the two
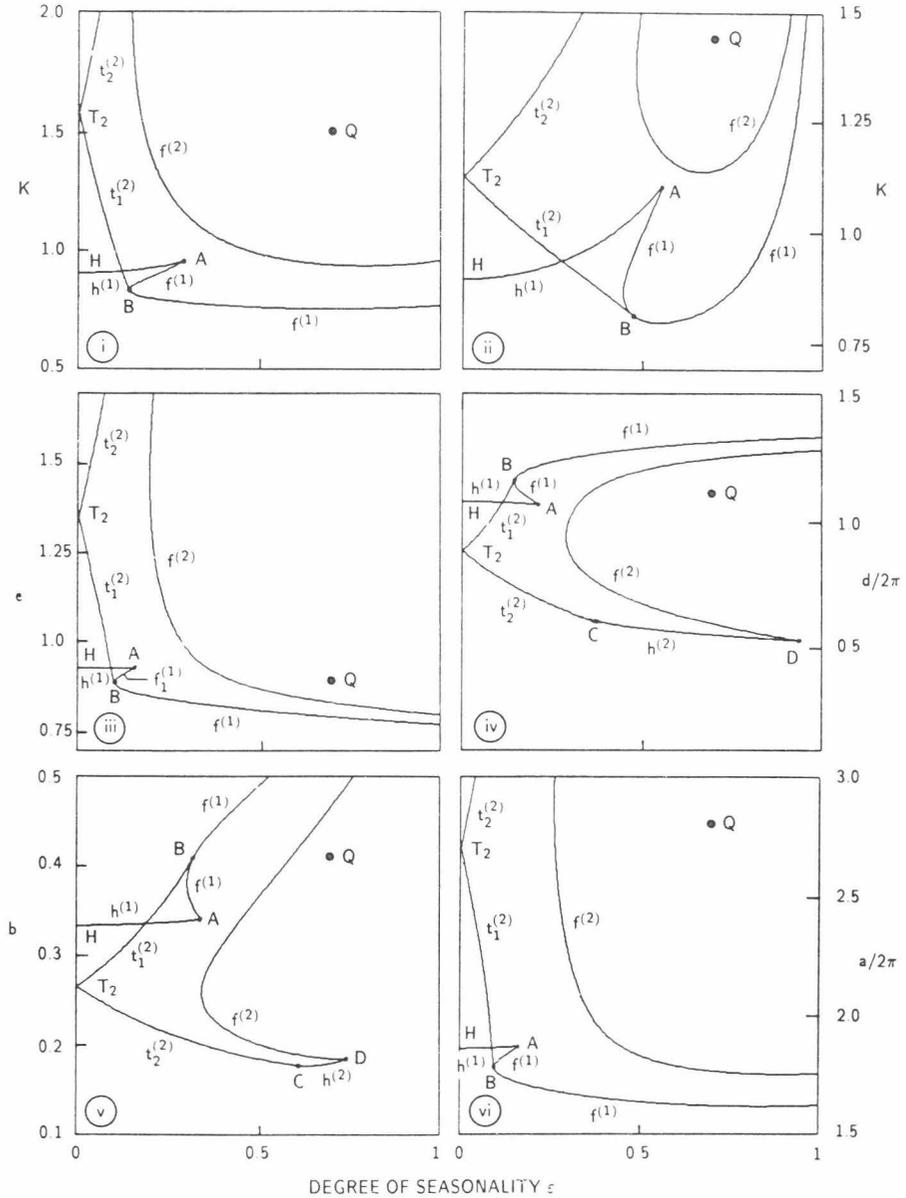
Figure 2. Bifurcation diagrams for system (1), (2). Each case (i), . . . , (vi) refers to the corresponding seasonality mechanism identified in Section 2. Curves $h^{(k)}$, $t^{(2)}$ and $f^{(k)}$, $k = 1$, 2 are Hopf, tangent and flip bifurcation curves, respectively. Points A, B, C, D are codimension two bifurcation points.

regions. When this curve is crossed from below, the forced stable cycle of period 1 smoothly bifurcates into a stable quasi-periodic solution. While continuing curve $h^{(1)}$ from the left to the right the multipliers $\mu^{(1)}_{1,2} = e^{\pm i\omega}$ of the Poincaré map vary and become equal to -1 when the terminal point A is reached.
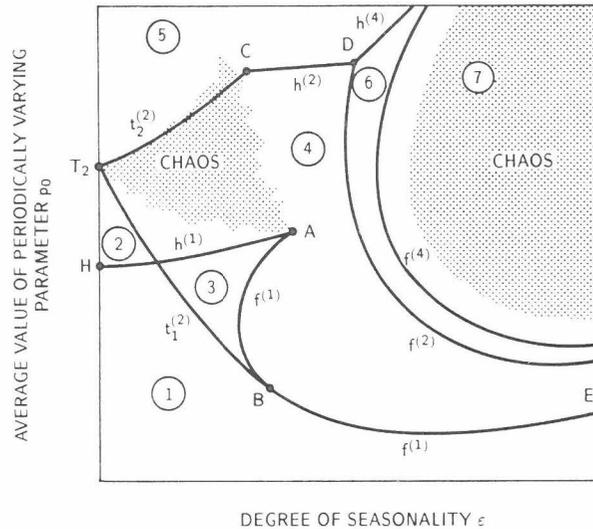
Figure 3. A general qualitative bifurcation diagram for systems (1), (2). Curves $h^{(1)}$, $h^{(2)}, h^{(4)}, f^{(1)}, f^{(2)}, f^{(4)}, t^{(2)}$ are bifurcation curves. Points A, B, C, D are codimension two bifurcation points.

Point A is a codimension two bifurcation point, called *strong resonance* 1:2, studied in Arnold (1982) by means of the normal form approach. The two coefficients of the normal form are of opposite sign and this suffices to say that only two bifurcation curves, namely, a Hopf $h^{(1)}$ and a flip $f^{(1)}$, are rooted at point A (as already said, the branch of $f^{(1)}$ not involving attractors is not shown in the figure). Curve $f^{(1)}$ can be generated by the continuation technique starting from point A. Along curve $f^{(1)}$ the normal form coefficient (computed as in Kuznetsov and Rinaldi, 1991) varies and becomes equal to 0 at point B, which is therefore a codimension two bifurcation point. Thus, curve $f^{(1)}$ is divided into two segments (AB and BE) and the period doubling takes place in opposite directions on these two segments, namely from region 4 on segment AB and from region 1 on segment BE. More precisely, when curve $f^{(1)}$ is crossed from region 1 to region 4 the forced cycle of period 1 loses stability and smoothly bifurcates into a stable period 2 cycle. On the contrary, if $f^{(1)}$ is crossed from region 3 to region 4, the stable cycle of period 1 collides with a saddle cycle of period 2 and becomes a saddle cycle of period 1.

The codimension two bifurcation point B is the terminal point of one of the

two branches of a tangent bifurcation curve $t^{(2)}$ (Afrajmovich *et al.*, 1991). The two branches $[t_1^{(2)}$ and $t_2^{(2)}]$ originate at point T_2 on the p_0-axis where the limit cycle of the unperturbed system has period 2. Some details concerning the system behaviour near point T_2 can be found in Guckenheimer and Holmes (1986). When $t_1^{(2)}$ and $t_2^{(2)}$ are crossed from the left, close to point T_2, a stable cycle of period 2 and a saddle cycle of period 2 appear. When branch $t_2^{(2)}$ is continued from point T_2 the first multiplier $\mu_1^{(2)}$ remains equal to 1 while the second $\mu_2^{(2)}$ varies smoothly and becomes equal to 1 at the codimension two bifurcation point C. After this point, the bifurcation curve $t_2^{(2)}$ does not involve attractors and has not been drawn in Fig. 3.

Point C is the root of a Hopf bifurcation curve $h^{(2)}$ ending at point D where the two multipliers are equal to -1 and the two coefficients of the normal form have the same sign. When $h^{(2)}$ is crossed from below, a stable cycle of period 2 bifurcates into an unstable cycle of period 2 and in a stable quasi-periodic solution.

Point D is the root of a bifurcation curve $f^{(2)}$ [and of a bifurcation curve $h^{(4)}$]. When curve $f^{(2)}$ is crossed from region 4 to region 6, a stable periodic solution of period 2 smoothly bifurcates into a stable periodic solution of period 4.

Finally, the analysis shows that flip bifurcation curves $f^{(4)}$, $f^{(8)}$ ... exist in the vicinity of curve $f^{(2)}$ [the difference between curves $f^{(2)}$ and $f^{(4)}$ is intentionally magnified in Fig. 3]. This cascade of period doublings results in strange attractors which can be found in some subregions of region 7.

The quasi-periodic solutions also bifurcate, but their bifurcation sets cannot be computed with our continuation technique. Nevertheless, in accordance with (Guckenheimer and Holmes, 1986), we can say that the stable quasi-periodic solution appearing on $h^{(1)}$ disappears through a homoclinic structure on a bifurcation set resembling a curve connecting point A with a point on branch $t_1^{(2)}$ close to point T_2. Thus, in this region we have strange attractors obtained through torus destruction (see Schaffer, 1988, Kuznetsov *et al.* 1992, for some examples).

Finally, we must point out that the same kind of bifurcations exist for cycles of period 3 (as well as for cycles of higher period). Indeed, two branches $t_1^{(3)}$ and $t_2^{(3)}$ of a tangent bifurcation originate at a point on the p_0-axis where the period of the limit cycle of the unperturbed system is equal to 3. When these branches are crossed from the left, a stable cycle of period 3 appears together with a saddle cycle of period 3. Then, the stable cycle undergoes a cascade of period doublings $f^{(3)}$, $f^{(6)}$, ... None of these bifurcation curves is shown in our figures in order to maintain them as readable as possible.

6. Multiple Attractors, Catastrophes and Chaos. The qualitative bifurcation diagram of Fig. 3 points out a number of interesting facts which prove that seasonalities can generate rather complex dynamics.

The first and most important fact is the existence of multiple attractors. Indeed, for a constant value of ε and for increasing values of p_0, a stable cycle of period 2 first coexists with a stable cycle of period 1 (in region 3 of Fig. 3), then with a quasi-periodic solution [in region 4, just above curve $h^{(1)}$] and, finally, with a strange attractor obtained through torus destruction (in a subregion of region 4). Coexistence of cycles of period greater than or equal to 3 with quasi-periodic solutions and strange attractors are also possible in the regions delimited by the branches $t_1^{(k)}$ and $t_2^{(k)}$, $k \geqslant 3$ of tangent bifurcation curves not shown in Fig. 3. Moreover, coexistence of triplets of attractors like, for example, cycles of period 2 and 3 and strange attractors, cannot be excluded although we have not found numerical evidence of it during our computational experiments.

A second relevant fact is that some of the bifurcations shown in Fig. 3 are catastrophic, so that even very small variations of a parameter can sometimes entail a radical change of behaviour of the system. Assume, for example, that the system behaves in region 1 of Fig. 3, just below the Hopf bifurcation curve $h^{(1)}$. In this region the system has only one stable mode of behaviour, namely a cycle of period 1. If p_0 is kept constant and ε is slowly increased, the stable cycle of period 1 varies smoothy but gradually loses stability when approaching the flip curve $f^{(1)}$. When line AB is crossed the attractor disappears because on that line the stable cycle of period 1 collides with a saddle cycle of period 2 and becomes a saddle cycle of period 1. Therefore, after $f^{(1)}$ has been crossed, the system moves toward another attractor, which, in the present case, is a period 2 cycle. After this catastrophic transition has occurred, the system is trapped in the new attractor. Indeed, even if ε is now slowly decreased, so that $f^{(1)}$ is crossed from the right, the stable mode of behaviour remains the cycle of period 2. Of course, if ε is further reduced, so that the tangent bifurcation curve $t_1^{(2)}$ is crossed from the right, we will have another catastrophic transition that brings the system back to a period 1 cycle. All this can be summarized by saying that if ε is alternatively increased and decreased so that curves $t_1^{(2)}$ and $f^{(1)}$ are crossed we will have a "hysteresis" involving transitions between cycles of period 1 and 2. Therefore, the catastrophic transitions characterizing the hysteresis involve a sudden variation of the frequency at which the system operates: a rather interesting behaviour.

Finally, the third important fact is the existence of deterministic chaos in two different regions of parameter space (see dotted regions of Fig. 3). The first region is characterized by relatively small values of ε and is delimited from below by the bifurcation set on which stable quasi-periodic solutions disappear through homoclinic structures (torus destruction). If p_0 is increased at constant ε starting from a point just above curve $h^{(1)}$ in Fig. 3, a small closed and regular curve on the Poincaré section (stable invariant torus) will first become bigger and bigger and then smoothly lose continuity and degenerate into a fractal

set (strange attractor). It is clear from Fig. 3 that these strange attractors can be present only for values of p_0 for which the unperturbed system behaves on a limit cycle. In other words, a predator–prey system which does not autonomously cycle in a constant environment, cannot become chaotic through torus destruction.

The second region of deterministic chaos is characterized by relatively high values of ε and corresponds to the second well-known route to chaos, namely cascade of period doublings $f^{(2)}, f^{(4)}, f^{(8)}, \ldots$. This region is delimited by a curve $f^{(\infty)}$ where the attractor loses periodicity and becomes chaotic. The curve $f^{(\infty)}$ cannot be found by numerical analysis because it is not possible to distinguish between a periodic cycle with an extremely large period and a genuine chaotic solution. Nevertheless, we can reasonably conjecture that curve $f^{(\infty)}$ is quite close to $f^{(2)}$ because the flip bifurcation curves $f^{(2)}, f^{(4)}, f^{(8)}, \ldots$ follow, in general, the Feigenbaum accumulation law (Guckenheimer and Holmes, 1986) and all our computations point out that $f^{(4)}$ and $f^{(8)}$ are already almost coinciding with $f^{(2)}$. Figure 4 shows six chaotic attractors, one for each seasonality mechanism, while Fig. 5 shows the corresponding time series of the y variable (predator) for a time interval equal to 25. All attractors have been obtained with the same degree of seasonality $\varepsilon = 0.7$ and with the other parameters (except the time varying ones) at their reference values (8). The corresponding points are denoted by Q in Fig. 2.

The analysis of Figs 2, 3 proves that the value of p_0 at which curve $f^{(\infty)}$ is minimum is sometimes lower than the value of p_0 corresponding to point H. This implies that this kind of chaotic behaviour can occur even if the corresponding unperturbed system does not autonomously cycle. The attractors (iii), (iv) and (v) of Fig. 4 are three examples. This characteristic allows one to further distinguish between the two types of chaos: the first (torus destruction) does not need high degrees of seasonality but requires a strong endogenous tendency to cycle, while the second (period doubling) requires high degrees of seasonality but can develop also in systems that would not cycle in a constant environment.

7. Concluding Remarks.   A classical predator–prey model has been studied in this paper with reference to the case of periodically varying parameters. Six elementary seasonality mechanisms have been identified and analysed in detail by means of a continuation technique automatically producing Hopf, tangent and flip bifurcation curves of periodic solutions of any period. The results have been compared and summarized through a general qualitative bifurcation diagram (Fig. 3) which allows one to classify and interpret the main modes of behaviour of the model. The general conclusion is that for suitable values of the parameters there are multiple attractors, catastrophes and strange attractors. Since, on the contrary, the unperturbed system has always a unique attractor
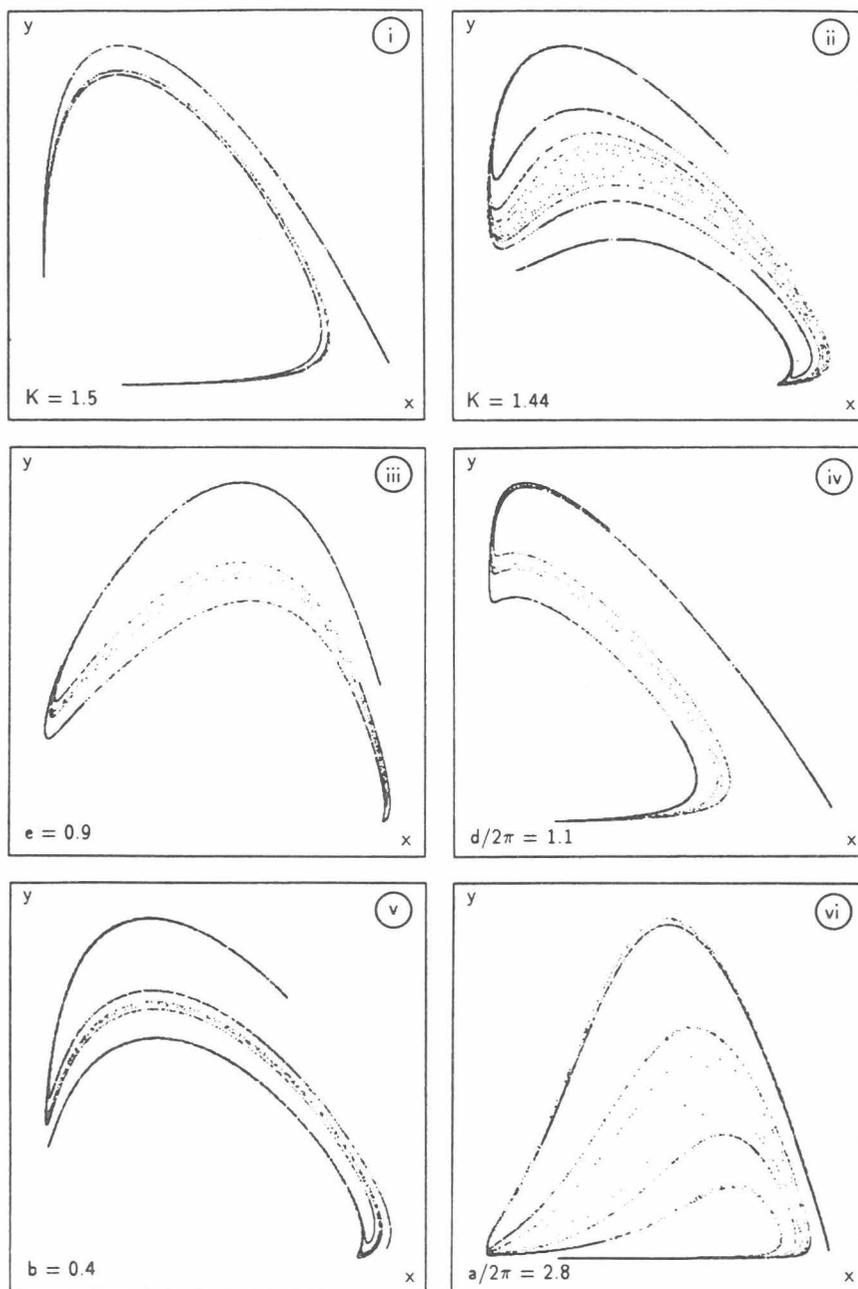
Figure 4. Strange attractors on the Poincaré section obtained through period doubling cascade. Each case (i), . . . , (vi) refers to the corresponding seasonality mechanism. All parameters, except those indicated on the figure, are at their reference values (8), and $\varepsilon = 0.7$.
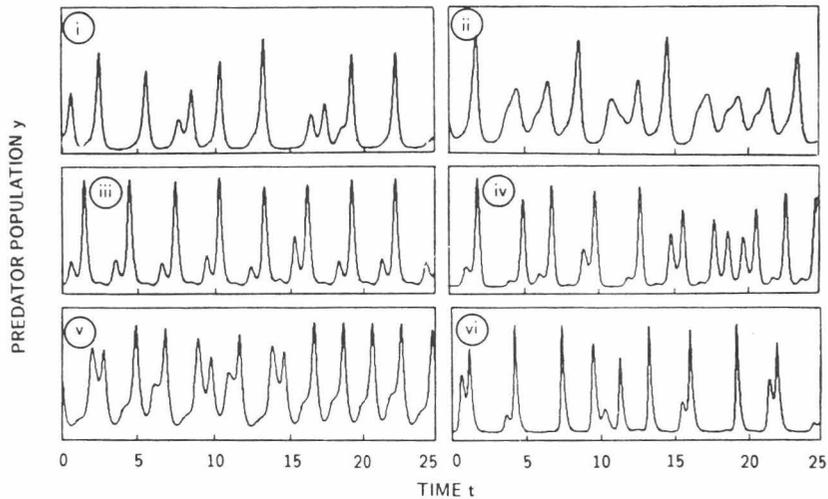
Figure 5. Normalized fluctuations of predator population y over a time period equal to 25. Each case (i), . . . , (vi) refers to the corresponding strange attractor of Fig. 4.

(an equilibrium or a limit cycle) our analysis proves that seasons can easily give rise to very complex predator–prey dynamics. This fact had already been established (Inoue and Kamifukumoto, 1984; Schaffer, 1988; Toro and Aracil, 1988; Allen, 1989) but not synthetically interpreted in terms of bifurcations, since the analysis was carried out only through simulation.

From a biological point of view the most interesting results are the following. If the degree of seasonality is small, the predator and the prey populations asymptotically vary in a periodic or in a quasi-periodic way. The period of the oscillations coincides with that of the forcing function (normalized to 1) if the system does not autonomously cycle when there are no seasons. On the contrary, if the unperturbed system behaves on a limit cycle, then the introduction of a small degree of seasonality transforms the cyclic behaviour into a quasi-periodic one. Moreover, in some subregions of the parameter space, there are also subharmonics, namely periodic solutions of period k times bigger than that of the forcing function ($k =$ integer). In particular, subharmonics of period 2 and 3 are relevant and have indeed been detected numerically in all cases we have analysed. Thus, multiplicity of attractors, for example coexistence of periodic solutions of period 2 or 3 and quasi-periodic solutions, is possible even at very low degrees of seasonality. This is also true for higher magnitudes of the seasonal variations at which, for example, subharmonics of period 2 can coexist with the basic period 1 solution (region 3 of Fig. 3). Actually, if the degree of seasonality is slowly varied and alternatively increased and decreased, the system can repeatedly undergo catastrophic transitions between periodic solutions of period 1 and 2 (hysteresis with frequency

switches). Finally, the two classical routes to chaos, i.e. torus destruction and cascade of period doublings, are present. Strange attractors of the first kind are obtained by introducing a low degree of seasonality in a predator–prey community which, in the absence of seasons, behaves on a limit cycle, while the second type of attractors can be generated, with a higher degree of seasonality, even when the system does not autonomously cycle. This means that chaos can be present in a predator–prey community provided that the exogenous and endogenous sources of periodicities are, as a whole, sufficiently strong.

As far as the method of analysis is concerned, we can summarize our experience by saying that continuation techniques producing bifurcation curves are very effective when they are used in conjunction with "detectors" of codimension two bifurcation points. Indeed, our bifurcation diagrams have been obtained in the following way. We have first generated curve $h^{(1)}$ starting from the Hopf bifurcation of the unperturbed system (point H in Fig. 3) and ending at point A, which is a codimension two bifurcation point. Then, we have produced the flip curve $f^{(1)}$, starting from point A, thus finding a second codimension two bifurcation point, namely point B. From this point we have generated the tangent bifurcation curve $t^{(2)}$ and found the third codimension two point, namely point C. Continuing like so, we have alternatively obtained bifurcation curves ($h^{(2)}$, $f^{(2)}$, $h^{(4)}$, $f^{(4)}$) and codimension two bifurcation points. Finding these codimension two points is therefore necessary for producing in a systematic way all the bifurcation curves. Of course, at each codimension two bifurcation point one must use the normal form approach to find out how many and which bifurcation curves are rooted at that point.For this reason we believe that packages which incorporate "detectors" and "analysers" of codimension two bifurcation points are very powerful for discussing the qualitative behaviour of nonlinear dynamical systems. More-over, they are the only serious tool for finding bifurcation curves which are not predicted by the available theories. For example, our bifurcation curves $f^{(2)}$ are not predicted by the known theory of periodically forced Hopf bifurcations (Kath, 1981; Rosenblat and Cohen, 1981; Gambaudo, 1985; Bajaj, 1986; Namachchivaya and Ariaratnam, 1987) (the interested reader can find more details on this matter in Kuznetsov *et al.*, 1992).

Although the analysis presented in this paper is quite detailed, we believe that there are still interesting questions to be answered and meaningful extensions to be performed. For example, it would be of interest to extend the analysis presented in this paper to predator–prey models which have also tangent and homoclinic bifurcations when they are not periodically perturbed. Among these models we have the case of a logistic prey, a Holling's type predator and a constant Holling's type superpredator, i.e. the most rudi-mentary food chain model (a more complete study of periodically forced food chain systems involving third order models appears to be very difficult because

such models can have chaotic behaviour even in the case of constant environment (Hogeweg and Hesper, 1978; Scheffer, 1990; Hastings and Powell, 1991). Another interesting extension would be to revisit the analysis of the periodically forced chemostat model carried out in (Kot *et al.*, 1992) with the use of circle maps. In fact, our continuation technique allows one to find codimension two bifurcation points and is therefore more powerful than the circle map technique. Finally, an interesting direction for further research is the investigation of the synergism among independent sources of periodicity. In particular, it would be interesting to know how chaos could be reinforced or damped by suitably "controlling" the phase between different elementary seasonality mechanisms. Information on this matter would be of particular relevance in the field of renewable resources management, where the time and intensity of stocking and harvesting must be well tuned with the natural periodicity mechanisms in order to avoid undesirable modes of behaviour.

LITERATURE

Afrajmovich, V. S., V. I. Arnold, Yu. S. Il'ashenko and P. Shilnikov. 1991. Bifurcation theory. In *Dynamical Systems*, Vol. 5, V. I. Arnold (Ed.), *Encyclopaedia of Mathematical Sciences*. New York: Springer Verlag.

Allen, J. C. 1989. Are natural enemy populations chaotic? In *Estimation and Analysis of Insect Populations*, *Lecture Notes in Statistics*, Vol. 55, L. McDonald, B. Manly, J. Lockwood and J. Logan (Eds), pp. 190–205. New York: Springer Verlag.

Arnold, V. I. 1982. *Geometrical Methods in the Theory of Ordinary Differential Equations*. New York: Springer Verlag.

Aron, J. L. and I. B. Schwartz. 1984. Seasonality and period-doubling bifurcations in an epidemic model. *J. theor. Biol.* **110**, 665–679.

Bajaj, A. K. 1986. Resonant parametric perturbations of the Hopf bifurcation. *J. Math. Anal. Appl.* **115**, 214–224.

Bardi, M. 1981. Predator–prey models in periodically fluctuating environments. *J. math. Biol.* **12**, 127–140.

Butler, G. J., S. B. Hsu and P. Waltman. 1985. A mathematical model of the chemostat with periodic washout rate. *SIAM J. appl. Math.* **45**, 435–449.

Cheng, K. S. 1981. Uniqueness of a limit cycle for a predator–prey system. *SIAM J. math. Anal.* **12**, 541–548.

Cushing, J. M. 1977. Periodic time-dependent predator–prey systems. *SIAM J. appl. Math.* **32**, 82–95.

Cushing, J. M. 1980. Two species competition in a periodic environment. *J. math. Biol.* **10**, 384–400.

Cushing, J. M. 1982. Periodic Kolmogorov systems. *SIAM J. math. Anal.* **13**, 811–827.

De Mottoni, P. and A. Schiaffino. 1981. Competition systems with periodic coefficients: a geometric approach. *J. math. Biol.* **11**, 319–335.

Gambaudo, J. M. 1985. Perturbation of a Hopf bifurcation by an external time-periodic forcing. *J. Diff. Eqns* **57**, 172–199.

Guckenheimer, J. and P. Holmes. 1986. *Nonlinear Oscillations, Dynamical Systems, and Bifurcations of Vector Fields.* New York: Springer Verlag.

Gutierrez, E. and H. Almiral. 1989. Temporal properties of some biological systems and their fractal attractors. *Bull. math. Biol.* **51**, 785–800.

Hastings, A. and T. Powell. 1991. Chaos in a three species food chain. *Ecology* **72**, 896–903.

Hogeweg, P. and B. Hesper. 1978. Interactive instruction on population interactions. *Comput. Biol. Med.* **8**, 319–327.

Holling, C. S. 1965. The functional response of predators to prey density and its role in mimicry and population regulation. *Mem. Entomol. Soc. Can.* **45**, 5–60.

Inoue, M. and H. Kamifukumoto. 1984. Scenarios leading to chaos in forced Lotka–Volterra model. *Prog. theor. Phys.* **71**, 930–937.

Kath, W. L. 1981. Resonance in periodically perturbed Hopf bifurcation. *Stud. Appl. Math.* **65**, 95–112.

Khibnik, A. I. 1990a. LINLBF: A program for continuation and bifurcation analysis of equilibria up to codimension three. In *Continuation and Bifurcations: Numerical Techniques and Applications*, D. Roose, B. de Dier and A. Spence (Eds), pp. 283–296. Netherlands: Kluwer Academic Publishers.

Khibnik, A. I. 1990b. Numerical methods in bifurcation analysis of dynamical systems: parameter continuation approach. In *Mathematics and Modelling.*, Yu. G. Zarhin and A. D. Bazykin (Eds), pp. 162–197. Pushchino: Center of Biological Research of the U.S.S.R. Academy of Sciences (in Russian).

Kot, M. and W. M. Schaffer. 1984. The effects of seasonality on discrete models of population growth. *Theor. pop. Biol.* **26**, 340–360.

Kot, M., W. M. Schaffer, G. L. Trutty, D. J. Grasser and L. F. Olsen. 1988. Changing criteria for imposing order. *Ecol. Model.* **43**, 75–110.

Kot, M., G. S. Sayler and T. W. Schultz. 1992. Complex dynamics in a model microbial system. *Bull. math. Biol.* **54**, 619–648.

Kuznetsov, Yu. A. and S. Rinaldi. 1991. Numerical analysis of the flip bifurcation of maps. *Appl. math. Comp.* **43**, 231–236.

Kuznetsov, Yu. A., S. Muratori and S. Rinaldi. 1992. *Bifurcations and chaos in a periodic predator–prey model. Int. J. Bifurcation Chaos* **2**, in press.

Lancaster, P. and M. Tismenetsky. 1985. *The Theory of Matrices.* San Diego: Academic Press.

Lauwerier, H. A. and J. A. J. Metz. 1986. Hopf bifurcation in host–parasitoid models. *IMA J. Math. appl. Med. Biol.* **3**, 191–210.

May, R. M. 1972. Limit cycles in predator–prey communities. *Science* **17**, 900–902.

May, R. M. 1974. Biological populations with nonoverlapping generations: stable points, stable cycles, and chaos. *Science* **186**, 645–647.

Metz, J. A. J. and F. H. D. van Batenburg. 1985. Holling's "hungry mantid" model for the invertebrate functional response considered as a Markov process. Part I: the full model and some of its limits. *J. math. Biol.* **22**, 209–238.

Namachchivaya, S. N. and S. T. Ariaratnam. 1987. Periodically perturbed Hopf bifurcation. *SIAM J. appl. Math.* **47**, 15–39.

Namba, T. 1986. Bifurcation phenomena appearing in the Lotka–Volterra competition equation: a numerical study. *Math. Biosci.* **81**, 191–212.

Olsen, L. F., G. L. Truty and W. M. Schaffer. 1988. Oscillations and chaos in epidemics: a nonlinear dynamic study of six childhood diseases in Copenhagen, Denmark. *Theor. pop. Biol* **33**, 344–370.

Robertson, D. R., C. W. Petersen and J. D. Brawn. 1990. Lunar reproductive cycles of benthic-broading reef fishes: reflections of larval biology or adult biology? *Ecol. Monogr.* **60**, 311–329.

Rosenblat, S. and D. S. Cohen. 1981. Periodically perturbed bifurcation—II Hopf bifurcation. *Stud. appl. Math.* **64**, 143–175.

Schaffer, W. M. 1984. Stretching and folding in Lynx fur returns: evidence for a strange attractor in nature? *Am. Nat.* **124**, 798–820.

Schaffer, W. M. 1988. Perceiving order in the chaos of nature. In *Evolution of Life Histories of Mammals*, M. S. Boyce (Ed.), pp. 313–350. New Haven: Yale University Press.

Scheffer, M. 1990. Should we expect strange attractors behind plankton dynamics and if so, should we bother? Ph.D. Thesis, University of Utrecht, The Netherlands (to be published in *J. Plankton Res.*).

Schwartz, I. B. and H. L. Smith. 1983. Infinite subharmonic bifurcation in an SEIR epidemic model. *J. math. Biol.* **18**, 233–253.

Smith, H. L. 1981. Competitive coexistence in an oscillating chemostat. *SIAM J. appl. Math.* **40**, 498–522.

Sugihara, G. and R. M. May. 1990. Nonlinear forecasting as a way of distinguishing chaos from measurement error in time series. *Nature* **344**, 734–741.

Toro, M. and J. Aracil. 1988. Qualitative analysis of system dynamics ecological models. *Syst. Dyn. Rev.* **4**, 56–80.

Verhulst, P. F. 1845. Recherches mathématiques sur la loi d'accroissement de la population. *Mem. Acad. r. Belg.* **18**, 1–38 (in French).

Wrzosek, D. M. 1990. Limit cycles in predator-prey models. *Math. Biosci.* **98**, 1–12.